

References

[1] K. Berg, P.K. Selbo, A. Weyergang, A. Dietze, L. Prasmickaite, A. Bonsted, B.O. Engesaeter, E. Angell-Petersen, T. Warloe, N. Frandsen, A. Hogset, Porphyrin-related photosensitizers for cancer imaging and therapeutic applications, *J. Microsc.* 218 (Pt 2) (2005) 133–147.

[2] S.K. Pushpan, S. Venkatraman, V.G. Anand, J. Sankar, D. Parmeswaran, S. Ganesan, T.K. Chandrashekar, Porphyrins in photodynamic therapy – a search for ideal photosensitizers, *Curr. Med. Chem. Anticancer Agents* 2 (2) (2002) 187–207.

[3] I. Rodica-Mariana, Synthetic metallo-porphyrins and selection criteria for PDT, *Oftalmologia* 56 (1) (2003) 83–88.

[4] S. Tsukagoshi, Development of a novel photosensitizer, talaporfin sodium, for the photodynamic therapy (PDT), *Gan To Kagaku Ryoho* 31 (6) (2004) 979–985.

[5] J. Usuda, H. Kato, T. Okunaka, K. Furukawa, H. Tsutsui, K. Yamada, Y. Suga, H. Honda, Y. Nagatsuka, T. Ohira, M. Tsuboi, T. Hirano, Photodynamic therapy (PDT) for lung cancers, *J. Thorac. Oncol.* 1 (5) (2006) 489–493.

[6] Y. Matsumura, H. Maeda, A new concept for macromolecular therapeutics in cancer chemotherapy: mechanism of tumor-tropic accumulation of proteins and the antitumor agent smancs, *Cancer Res.* 46 (12 Pt 1) (1986) 6387–6392.

[7] H. Maeda, Macromolecular therapeutics in cancer treatment: the EPR effect and beyond, *J. Control. Release* 164 (2) (2012) 138–144.

[8] H. Maeda, Y. Matsumura, EPR effect based drug design and clinical outlook for enhanced cancer chemotherapy, *Adv. Drug Deliv. Rev.* 63 (3) (2011) 129–130.

[9] H. Maeda, Tumor-selective delivery of macromolecular drugs via the EPR effect: background and future prospects, *Bioconjug. Chem.* 21 (5) (2010) 797–802.

[10] H. Maeda, Vascular permeability in cancer and infection as related to macromolecular drug delivery, with emphasis on the EPR effect for tumor-selective drug targeting, *Proc. Jpn. Acad. Ser. B Phys. Biol. Sci.* 88 (3) (2012) 53–71.

[11] H. Maeda, in: *Polymer Conjugated Macromolecular Drugs for Tumor-specific Targeting*, John Wiley & Sons Ltd, New York, 1994, pp. 353–382.

[12] Y. Noguchi, J. Wu, R. Duncan, J. Strohal, K. Ulbrich, T. Akaike, H. Maeda, Early phase tumor accumulation of macromolecules: a great difference in clearance rate between tumor and normal tissues, *Jpn. J. Cancer Res.* 89 (3) (1998) 307–314.

[13] L.W. Seymour, Y. Miyamoto, H. Maeda, M. Brereton, J. Strohal, K. Ulbrich, R. Duncan, Influence of molecular weight on passive tumour accumulation of a soluble macromolecular drug carrier, *Eur. J. Cancer* 31A (5) (1995) 766–770.

[14] C. He, Y. Hu, L. Yin, C. Tang, C. Yin, Effects of particle size and surface charge on cellular uptake and biodistribution of polymeric nanoparticles, *Biomaterials* 31 (13) (2010) 3657–3666.

[15] T. Etrych, P. Chytil, T. Mrkvan, M. Sirova, B. Rihova, K. Ulbrich, Conjugates of doxorubicin with graft HPMA copolymers for passive tumor targeting, *J. Control. Release* 132 (3) (2008) 184–192.

[16] K. Ulbrich, T. Etrych, P. Chytil, M. Jelinkova, B. Rihova, HPMA copolymers with pH-controlled release of doxorubicin: in vitro cytotoxicity and in vivo antitumor activity, *J. Control. Release* 87 (1–3) (2003) 33–47.

[17] F.M. Veronese, G. Pasut, PEGylation, successful approach to drug delivery, *Drug Discov. Today* 10 (21) (2005) 1451–1458.

[18] A.K. Iyer, K. Greish, T. Seki, S. Okazaki, J. Fang, K. Takeshita, H. Maeda, Polymeric micelles of zinc protoporphyrin for tumor targeted delivery based on EPR effect and singlet oxygen generation, *J. Drug Target.* 15 (7–8) (2007) 496–506.

[19] M. Regehly, K. Greish, F. Rancan, H. Maeda, F. Bohm, B. Roder, Water-soluble polymer conjugates of ZnPP for photodynamic tumor therapy, *Bioconjug. Chem.* 18 (2) (2007) 494–499.

[20] J. Fang, T. Sawa, T. Akaike, T. Akuta, S.K. Sahoo, G. Khaled, A. Hamada, H. Maeda, In vivo antitumor activity of pegylated zinc protoporphyrin: targeted inhibition of heme oxygenase in solid tumor, *Cancer Res.* 63 (13) (2003) 3567–3574.

[21] S.K. Sahoo, T. Sawa, J. Fang, S. Tanaka, Y. Miyamoto, T. Akaike, H. Maeda, Pegylated zinc protoporphyrin: a water-soluble heme oxygenase inhibitor with tumor-targeting capacity, *Bioconjug. Chem.* 13 (5) (2002) 1031–1038.

[22] A.K. Iyer, K. Greish, J. Fang, R. Murakami, H. Maeda, High-loading nanosized micelles of copoly(styrene-maleic acid)-zinc protoporphyrin for targeted delivery of a potent heme oxygenase inhibitor, *Biomaterials* 28 (10) (2007) 1871–1881.

[23] J. Fang, K. Greish, H. Qin, L. Liao, H. Nakamura, M. Takeya, H. Maeda, HSP32 (HO-1) inhibitor, copoly(styrene-maleic acid)-zinc protoporphyrin IX, a water-soluble micelle as anticancer agent: in vitro and in vivo anticancer effect, *Eur. J. Pharm. Biopharm.* 81 (3) (2012) 540–547.

[24] H. Maeda, Assay of proteolytic enzymes by the fluorescence polarization technique, *Anal. Biochem.* 92 (1) (1979) 222–227.

[25] H. Nakamura, J. Fang, B. Gahininath, K. Tsukigawa, H. Maeda, Intracellular uptake and behavior of two types zinc protoporphyrin (ZnPP) micelles, SMA-ZnPP and PEG-ZnPP as anticancer agents; unique intracellular disintegration of SMA micelles, *J. Control. Release* 155 (3) (2011) 367–375.

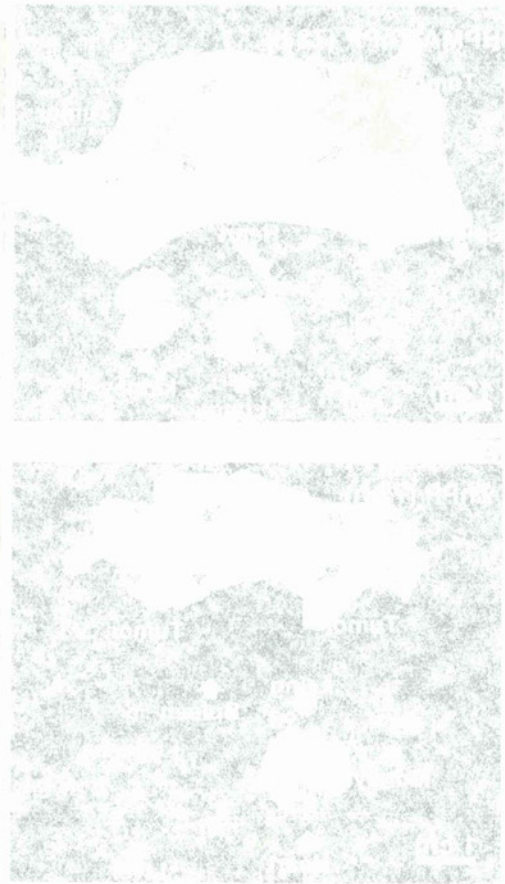
[26] H.P. Kim, H.O. Pae, S.H. Back, S.W. Chung, J.M. Woo, Y. Son, H.T. Chung, Heme oxygenase-1 comes back to endoplasmic reticulum, *Biochem. Biophys. Res. Commun.* 404 (1) (2011) 1–5.

[27] T. Linden, J. Doutheil, W. Paschen, Role of calcium in the activation of erp72 and heme oxygenase-1 expression on depletion of endoplasmic reticulum calcium stores in rat neuronal cell culture, *Neurosci. Lett.* 247 (2–3) (1998) 103–106.

[28] J. Fang, T. Akaike, H. Maeda, Antiapoptotic role of heme oxygenase (HO) and the potential of HO as a target in anticancer treatment, *Apoptosis* 9 (1) (2004) 27–35.

[29] J. Fang, H. Nakamura, H. Maeda, The EPR effect: unique features of tumor blood vessels for drug delivery, factors involved, and limitations and augmentation of the effect, *Adv. Drug Deliv. Rev.* 63 (3) (2010) 136–151.

[30] H. Maeda, G.Y. Bharate, J. Daruwalla, Polymeric drugs for efficient tumor-targeted drug delivery based on EPR-effect, *Eur. J. Pharm. Biopharm.* 71 (3) (2009) 409–419.





The EPR effect for macromolecular drug delivery to solid tumors: Improvement of tumor uptake, lowering of systemic toxicity, and distinct tumor imaging in vivo[☆]

Hiroshi Maeda^{*}, Hideaki Nakamura, Jun Fang

DDS Research Institute, Sojo University, 4-22-1, Ikeda, Kumamoto, 860-0082, Japan

ARTICLE INFO

Article history:

Accepted 16 October 2012

Available online 23 October 2012

Keywords:

EPR effect mediators
Enhancement of the EPR effect
Tumor-selective drug delivery
Inflammation
Cancer
Vascular effectors
Fluorescent nanoprobosc
Tumor blood vessel architecture

ABSTRACT

The EPR effect results from the extravasation of macromolecules or nanoparticles through tumor blood vessels. We here provide a historical review of the EPR effect, including its features, vascular mediators found in both cancer and inflamed tissue. In addition, architectural and physiological differences of tumor blood vessels vs that of normal tissue are commented. Furthermore, methods of augmentation of the EPR effect are described, that result in better tumor delivery and improved therapeutic effect, where nitroglycerin, angiotensin I-converting enzyme (ACE) inhibitor, or angiotensin II-induced hypertension are employed. Consequently, better therapeutic effect and reduced systemic toxicity are generally observed. Obviously, the EPR effect based delivery of nanoprobosc are also useful for tumor-selective imaging agents with using fluorescent or radio nuclei in nanoprobosc. We also commented a key difference between passive tumor targeting and the EPR effect in tumors, particularly as related to drug retention in tumors: passive targeting of low-molecular-weight X-ray contrast agents involves a retention period of less than a few minutes, whereas the EPR effect of nanoprobosc involves a prolonged retention time—days to weeks.

© 2012 Elsevier B.V. All rights reserved.

Contents

| | |
|--|----|
| 1. Introduction: vascular permeability in inflammation and cancer | 71 |
| 2. Vascular effectors involved in vascular permeability in cancer and inflammation | 73 |
| 3. Revisiting the definition of the EPR effect: molecular size, biocompatibility, and surface charge | 73 |
| 3.1. Biocompatibility and molecular size | 73 |
| 3.2. Surface charge | 74 |
| 3.3. Hydrophobicity | 74 |
| 4. Defective architecture of tumor blood vessels and lymphatic function | 74 |
| 5. Augmentation of the EPR effect and macromolecular drug delivery to tumors | 75 |
| 6. Fluorescence imaging and the EPR effect with fluorescent nanoprobosc | 76 |
| 7. Conclusions | 78 |
| References | 78 |

Abbreviations: NO, nitric oxide; MMP, matrix metalloproteinase; EPR effect, enhanced permeability and retention effect; VPF, vascular permeability factor; VEGF, vascular endothelial growth factor; e-NOS, endothelial nitric oxide synthase; ACE, angiotensin converting enzyme; TNF- α , tumor necrosis factor- α ; SMA, styrene-co-maleic acid; AT-II, angiotensin II; i.v., intravenous; DTPA, diethylenetriaminepentaacetic acid; BSA, bovine serum albumin; TRITC, tetramethylrhodamine isothiocyanate; ICG, indocyanine green; HPMA, N-(2-hydroxypropyl)methacrylamide.

[☆] This review is part of the *Advanced Drug Delivery Reviews* theme issue on "25th Anniversary issue — Advanced Drug Delivery: Perspectives and Prospects".

^{*} Corresponding author. Tel.: +81 96 326 4114; fax: +81 96 326 3185.

E-mail address: hirmaeda@ph.sojo-u.ac.jp (H. Maeda).

1. Introduction: vascular permeability in inflammation and cancer

About 30 years ago, we first discovered that vascular permeability in inflammation, that was induced by microbial infections, and triggered by bradykinin (kinin) generation via activation of the proteolytic cascade in the host animals (Fig. 1) [1–5]. We later found that bradykinin was also generated in carcinomatosis and found it was responsible for ascitic and pleural fluid accumulation [6–8]. In addition, we identified many other mediators that were activated simultaneously [9–15], including nitric oxide (NO), prostacyclins, collagenase, and peroxyinitrite, which activate matrix metalloproteinase (MMP) (via pro-MMP) and others [11–15].

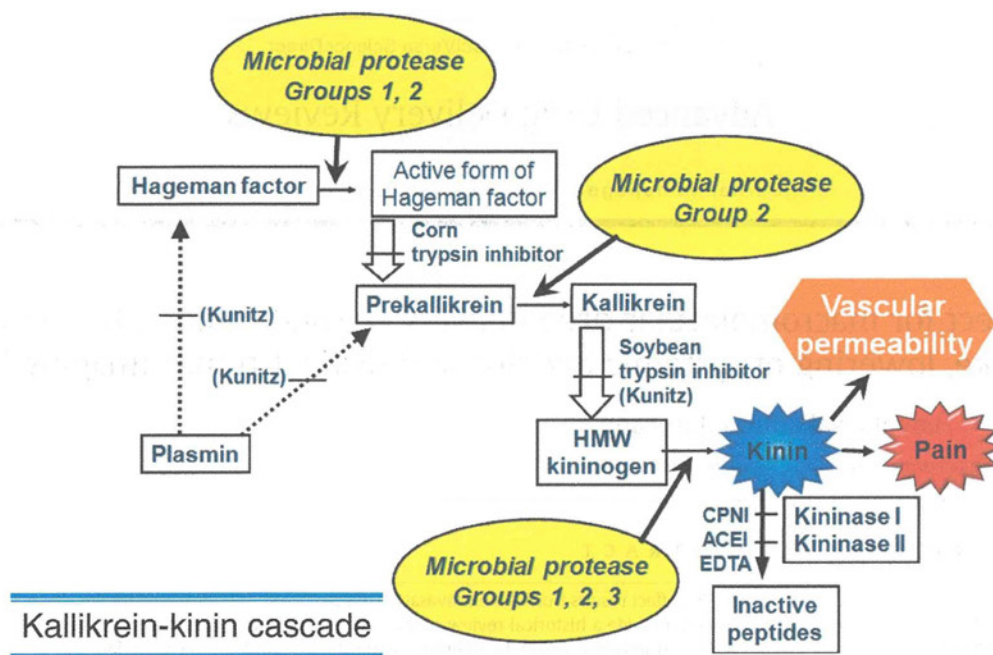


Fig. 1. The bradykinin-generating protease cascade, which is triggered by bacterial proteases followed by activation of the kallikrein-kinin cascade. The same bradykinin-generating mechanism operates in cancer tissue and in inflamed tissue. A number of protease inhibitors, such as Kunitz-type soybean trypsin inhibitor (Kunitz), corn trypsin inhibitor (Corn), carboxypeptidase N inhibitor (CPNI), angiotensin-converting enzyme inhibitor (ACEI), and ethylenediaminetetraacetic (EDTA) inhibit these cascade steps, or consequently potentiate kinin (e.g. ACEI).

We published many reports on the new concept of macromolecular cancer drug delivery, which we named the enhanced permeability and retention (EPR) effect for tumor-selective macromolecular drug targeting [16–23]. Vascular permeability of tumor tissue thus became critically important for the delivery of macromolecular drug based on the EPR effect in cancer treatment.

Fig. 2 presents the various steps involved in drug delivery to tumor tissues and then to tumor cells, and they are the barriers that must be overcome in cancer drug development. The EPR effect, at the first step, is of prime importance because drug extravasation occurs in a

tumor-selective manner. Traditional low-molecular-weight (LMW) anti-cancer drugs have very little tumor selectivity, and most such drugs are widely distributed to normal organs and tissues as well as tumors. Consequently, these anticancer drugs provide insufficient therapeutic benefits and cause severe systemic toxicity, a so-called dose-limited toxicity. By developing tumor-selective anticancer agents, we can avoid this problem.

The present review is intended to overview various aspects of the EPR effect. To demonstrate the EPR effect visually *in vivo*, tumor selective imaging using fluorophore that is conjugated with macromolecules (fluorescent nanoprobes) and IVIS® imaging system are described later.

| Steps | Barriers to be overcome | Comments |
|-----------------|--|--|
| 1 st | Vascular wall /Circulating Blood EPR effect / Extravasation into tumor tissue ↓ Tumor tissue/Interstitial space | Polymeric drugs/nanomedicines Vascular wall openings Enhancement of the EPR effect by NO and angiotensin-converting enzyme inhibitor |
| 2 nd | Dissemination to tumor cells ↓ | Stromal matrix/fibrin gel/fibroblast: protease/plasmin/plasminogen activator |
| 3 rd | Cell membrane/ internalization ↓ | Endocytic uptake Styrene-co-maleic acid (SMA) micelle disintegration |
| 4 th | Drug release /free active drug pH/protease-labile linker Interact with target molecules ↓ | No exocytosis Hydrazone/maleic acid help drug release |
| 5 th | In vivo antitumor effect: 100% survival/cure ↓ | React with target molecules High antitumor efficacy <i>in vivo</i> |
| 6 th | Regulatory steps/safety issue ↓ | Phase I, II, III trials |
| 7 th | Cost/benefit | More universal tumor targets [Evaluation by Natl. Inst. Health Clin. Excellence, UK] |

Fig. 2. Barriers in the development of cancer selective macromolecular drugs and steps to be overcome.

Advantages of this EPR based macromolecular cancer therapy, without using targeting ligand, is more universal and can be applied to wider tumor spectrum than that using a tumor associated epitope-targeted antibody. In the clinical setting, specific target epitopes of different tumors may be unidentified at early stage of diagnosis. Thus, such therapeutic or diagnostic method may not be as easy as endoscopic visual detection which may be possible with using fluorescent nanoprobe as described later.

In the past few decades numerous papers were published for tumor targeted delivery of drugs, and imaging using either positron emitting tomography (PET), magnetic resonance imaging (MRI), or fluorescent imaging with fluorophores. Since all these nanoprobe exhibit the EPR effect, such developments are highly advantageous in more efficient treatment and sensitive diagnosis of tumor and inflamed tissues respectively [24–37]. More comprehensive treatise on all these issues may be found in references [31,37].

2. Vascular effectors involved in vascular permeability in cancer and inflammation

Most of these effectors are common mediators in inflammation and cancer (Fig. 3, Table 1) [11–15,17–19] and are highly expressed. Senger et al. [38] and Dvorak et al. [39] found the cancer-specific vascular permeability factor (VPF), which was secreted by tumor cells. VPF was later identified as vascular endothelial growth factor (VEGF) [15,40–42], which in fact enhances the vascular permeability of normal blood vessels as well as that of tumor vessels [15,17], with this process partly involving endothelial nitric oxide synthase (e-NOS) and thus NO.

Bradykinin (kinin) and inhibitors of the kinin-degrading enzyme (kininase), such as angiotensin converting enzyme (ACE) inhibitor [5–8,22], potentiated vascular permeability and the EPR effect. Likewise, generation of oxygen radicals and NO, which is induced during microbial infection and inflammation [10,11,43–45], augmented the EPR effect in cancer. In addition, hypoxic cancer tissues and angina pectoris (or cardiac infarction) demonstrated marked similarity with regard to suppressed vascular blood flow. This observation led to the use of nitroglycerin treatment to improve vascular blood flow and consequently the EPR effect (Fig. 4) [46,47].

These vascular mediators, including activated cyclooxygenase-1, interferon- γ , and inducible NOS (iNOS), as well as other cytokines such as tumor necrosis factor- α (TNF- α), transforming growth factor- β , and interleukin-2 and -8 etc., display cross-talks [15–18,48–53].

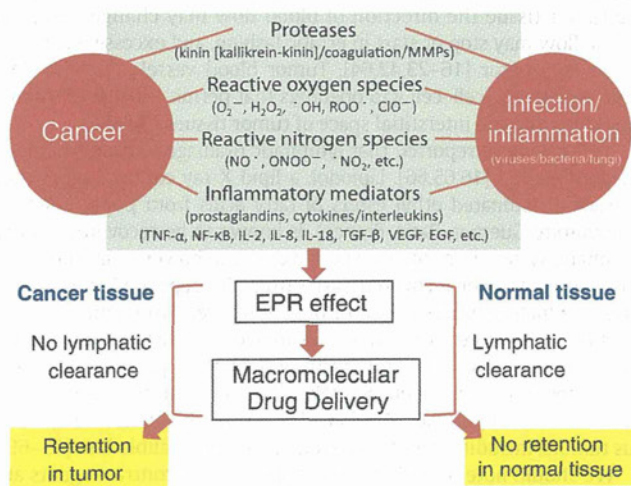


Fig. 3. Various vascular mediators commonly found in inflammation and cancer that contribute to the EPR effect. These mediators also affect normal blood vessels. A major difference between the two pathological lesions is the clearance rate of extravasated macromolecules such as plasma proteins, lipid particles or nanomedicine, which resulting in a prolonged retention time in tumor tissue compared with that in inflamed tissue.

Table 1
Factors affecting the EPR effect of macromolecular drugs in solid tumors.^a

| Mediators | Responsible enzymes and mechanisms |
|---|---|
| Bradykinin | Kallikrein/protease |
| NO | iNOS |
| VPF/VEGF | Involved in NO generation |
| Prostaglandins | Cyclooxygenase 1 |
| Collagenase (MMPs) | Activated from proMMPs by peroxynitrite, or proteases |
| Peroxyntirite | NO + O ₂ ^{·-} |
| Carbon monoxide (CO) ⁷⁶ | Heme oxygenase (HO)-1 |
| Induced hypertension | Using angiotensin II |
| Inflammatory cells and H ₂ O ₂ | Neutrophil/NADPH oxidase, etc. |
| Transforming growth factor (TGF)- β inhibitor ⁷⁷ | |
| Tumor necrosis factor (TNF)- α ⁷⁸ | |
| Anticancer agents | |
| Heat ³⁶ | |

^a Extensive production of vascular mediators that facilitate extravasation from normal and tumor vessels, and the enzymes and mechanisms involved in this process (see text for more details).

3. Revisiting the definition of the EPR effect: molecular size, biocompatibility, and surface charge

3.1. Biocompatibility and molecular size

Among the various requirements for and factors influencing the EPR effect, the most important is having a molecular size larger than 40 kDa (Fig. 5, Table 2) [9,16–23,42]. However, this requirement is only partly valid, because size alone is not sufficient for the EPR effect to occur. Biocompatibility may predominate (see Table 2). For instance, most native plasma proteins have a plasma half-life of more than a few days. In contrast, denatured or highly chemically modified plasma proteins are cleared very rapidly. As another example, α_2 -macroglobulin (a tetramer of 170 kDa) is an endogenous protease inhibitor in the blood that has a half-life of more than several days. However, the complex of α_2 -macroglobulin with plasmin, which is an endogenous serine-type protease that is involved in fibrinolysis, has a half-life of only about 5 min and is cleared very rapidly from the circulation (Table 3) [53,54]. Likewise, certain chemical modifications of albumin result in a much shorter plasma half-life (Table 3).

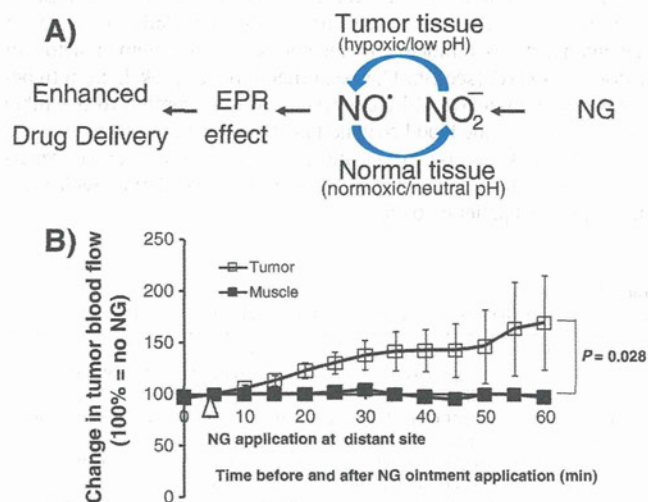


Fig. 4. (A) Mechanism of NO generation from the nitro agents, nitroglycerin (NG). NO was generated from nitrite, predominantly in hypoxic tumor tissues, not in normal tissues. (B) NG enhanced blood flow seen only in tumor tissue, not in normal tissue. Sarcoma 180 tumor-bearing mice with tumor diameters of 6–7 mm were anesthetized, and the blood flow was measured with a laser flow meter. In this experimental setting, accumulation of the Evans blue-albumin complex increased 2- to 3-fold more than without NG (see text). Adapted from ref. [46].

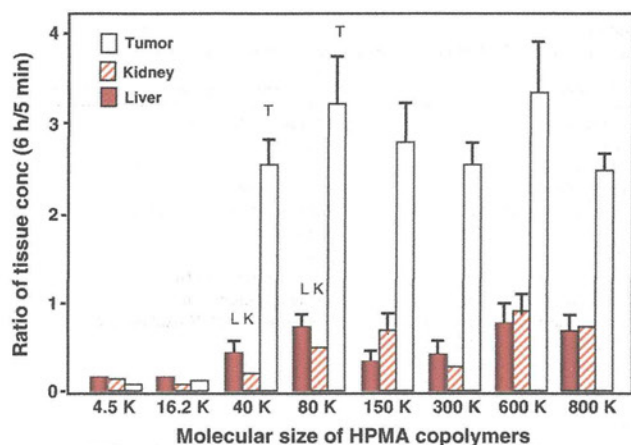


Fig. 5. Tumorotropic uptake of the biocompatible macromolecules, *N*-(2-hydroxypropyl) methacrylamide (HPMA) polymers containing radioactive ¹³¹I-labeled tyrosine were used for this study. The EPR effect leading to higher uptake of the HPMA polymer into tumors is seen for polymer sizes larger than 40 kDa. The amount of uptake at 6 h is compared with that at 5 min. That is, tumor uptake increases with time. Adapted from ref. [20].

This finding suggests the possibility that active ligand-conjugated antibodies will be cleared from the circulation much faster than native proteins or even unmodified biocompatible polymers. This possibility may pose a problem in that an active ligand-targeting strategy and ligand-conjugated product (conjugates) may cause shortened plasma half-lives, the result being not enough time for the EPR effect, which requires a long circulation time.

3.2. Surface charge

The luminal surface of blood vessels is well known to have a negatively charged surface, such as many sulfated and carboxylate sugar moieties [55]. This characteristic means that polymeric drugs with high positive charges will bind nonspecifically to the luminal surface of vascular walls and be rapidly cleared from the blood circulation (Table 4) [56,57]. Particles with high negative charges, however, are known to be trapped in the liver. Also, particles with high negative charges on the solid surface will trigger the coagulation cascade, *i.e.* Hageman factor is stimulated to become activated Hageman factor (or factor XII → XIIα) (see Fig. 1), which then induces prekallikrein to become kallikrein, followed by conversion of prothrombin to thrombin and activation of the blood coagulation (blood clotting) cascade. Blood coagulation has serious clinical consequences. In the worst case scenario, it may result in disseminated intravascular coagulation, which frequently causes patients to die.

Table 2
Characteristics of the EPR effect of nanomedicines and macromolecular drugs.

| | |
|--------------------------|---|
| Biocompatibility | No interaction with blood components or blood vessels, no antigenicity, no clearance by the reticuloendothelial system, no cell lysis |
| Molecular size | Larger than 40 kDa (larger than the renal clearance threshold) |
| Surface charge | Weakly negative to near neutral |
| Time required to achieve | Longer than several hours in systemic circulation in mice, with distinct accumulation seen at 30 min ^{16,20} |
| Drug retention time | Usually days to weeks, in great contrast to passive targeting, in which low-molecular-weight molecules are rapidly cleared and enter the systemic circulation in a few minutes (compare with low-molecular-weight contrast agents) ^a |

^a Compare with low-molecular-weight (LMW) contrast agents in angiography, which is taken up in the tumor tissue by passive targeting, but not retained (see text). Arterial injection of LMW anticancer agents, though they hit tumor by the first pass effect, it is not retained in tumor tissue, and so there is not much clinical benefit.

3.3. Hydrophobicity

An important aspect of hydrophobicity is that an increase in hydrophobicity of nanoparticles would result in higher affinity to a cell membrane [58a], and also a much faster endocytotic uptake in parallel with an increase of the cell-association constant to about 10–100 fold [58a,58b]. Further, the environment or pH responsive character of polymeric drugs can be added by utilizing, for instance, maleyl carboxyl group (*i.e.* hydrophilic-COO⁻ of neutral pH to hydrophobic-COOH at weakly acidic pH) as seen in an SMA-conjugate [58b,58c]. This became more apparent when compared with SMA-micelles vs PEG-conjugated micelles as SMA-micelles were endocytosed about 10 times more than the others [58d].

Hydrophobic polymers with high affinity to cell membranes should also be tested with red blood cells to investigate hemolysis. Also, solubility will be lower as hydrophobicity increases or more side chains are introduced, as we experienced with styrene-co-maleic acid (SMA) copolymer [58a,59]. However, hydrophobicity can be significantly modified by introducing hydrophilic side chain residues, and polymers will become less hemolytic, as we observed with various SMA copolymers.

Another advantage of hydrophobic polymer derivatization is that one can make oily formulation possible. In case of SMANCS, its oily formulation made much higher absorbability after oral administration (×17 times). This indicates one can make peptidic drugs for oral administration possible by this way [58e].

It should be mentioned that the evaluation of polymeric and nanoparticle drugs for their effect on hemolysis, coagulation, and stability in fresh blood at the early stage of drug development should be carried out for a safely point of view (*e.g.* ref. [58a]).

4. Defective architecture of tumor blood vessels and lymphatic function

Folkman first documented active angiogenesis in solid tumor many years ago [40,41]. Electron microscopy of a vascular cast of tumor blood vessels that was obtained by using polymer resin showed clear differences between tumor vessels and normal blood vasculature [60–62]. Also, the blood flow volume in tumor tissue is markedly different from that in normal tissue. As noted later in this article (next section), the blood flow volume in normal tissue is consistent, regardless to the blood pressure being modulated by infusion of angiotensin II. However, in tumor tissue, blood flow volume changes (increases) remarkably as angiotensin II is infused to achieve higher blood pressure [63]. Also, in the tumor tissue the direction of blood flow may change abruptly, *i.e.* the flow may stop or start in erratic fashion, and excessive extravasation may occur [16–23,42,64]. Tumor blood vessels also manifest large endothelial cell–cell gap openings that permit leakage of macromolecules into the interstitial space of tumor tissues [60–62].

We previously reported that lymphatic drainage in tumor tissue is highly impaired [16,65,66]. Lipiodol, a lipid X-ray contrast agent that consists of iodinated ethyl esters of fatty acids from poppy seed oil (Laboratoire Guerbet, Paris, France), is known to be recovered via the lymphatic system in normal tissues. In contrast, however, in tumor tissues, Lipiodol is not recovered easily from the deposited site (cancer tissue), which indicates a lack of or an impaired lymphatic recovery function. Therefore, we took advantage of this tumor-specific retention of Lipiodol for administration of the lipophilic polymer-conjugated anticancer agent SMANCS [neocarzinostatin (NCS) conjugated with the copolymer SMA] in a Lipiodol formulation to treat various tumors, including cancers of liver, kidney, and gallbladder [65–69].

We should note here that water-soluble LMW contrast agents are also taken up preferentially by highly vascularized tumors when infused into the tumor-feeding artery. This technique is used in arterial angiography. Although tumor-selective retention of these LMW contrast agents, or likewise LMW anticancer agents, is observed, that is often called passive tumor-targeting, but it lasts no longer than a

Table 3
Plasma clearance times of selected modified and native proteins in vivo [53,54].^a

| Protein | Species difference, original/test | Probe modification | pI | MW (kDa) | t _{1/2} |
|---|-----------------------------------|---------------------------------------|------|----------|------------------|
| | | | | | |
| Albumin | Mouse/mouse | None | 4.8 | 68 | 72–96 h |
| Albumin | Mouse/mouse | DTPA (⁵¹ Cr) | ≤4.8 | – | 6 h |
| Albumin | Cow/mouse | DTPA (⁵¹ Cr) | ≤4.8 | – | 1 h |
| Formaldehyde-modified albumin | Human/rat | ¹²⁵ I-labeled formaldehyde | ≤4.8 | – | 25 min |
| α ₂ -Macroglobulin | Human/mouse | ¹²⁵ I | 5.3 | 180×4 | 140 h |
| α ₂ -Macroglobulin-plasmin complex | Human/mouse | ¹²⁵ I | – | 180×4 | 5 min |
| Immunoglobulin (IgG) | Mouse/mouse | DTPA | ≤6.8 | 159 | 60 h |
| IFN-α | Human/human | None | – | 18 | 8 h (sc) |
| PEG-IFN-α2a | Human/human | PEG | – | 52 | 80 h (sc) |

^a DTPA, diethylenetriaminepentaacetic acid; IFN, interferon; PEG, polyethylene glycol; sc, given subcutaneously.

few minutes. This characteristic of short time period is in great contrast to that for the EPR effect, in which retention of the lipid particles of Lipiodol or macromolecular drugs persists for a long time, for a few weeks to months [16–18,22,23,42,65–69]. Thus, in contrast to polymeric drugs such as SMANCS/Lipiodol, the LMW contrast agents, or likewise LMW anticancer agents may demonstrate only passive tumor targeting for a very short time, but they will not be retained for substantial periods (e.g. days to weeks).

5. Augmentation of the EPR effect and macromolecular drug delivery to tumors

As Table 1 shows, we and others have identified permeability factors, such as bradykinin, NO, and prostaglandins, that facilitate extravasation or the EPR effect in cancer tissues. Generation of these factors does not occur in normal benign tissues, namely, these systems are not activated under normal circumstances. Therefore, augmentation of these factors will affect only tumor or inflamed tissues, with the results being tumor-selective enhanced vascular permeability and improved delivery of drugs to tumors. Nitroglycerin [46,47] and other NO-releasing agents such as isosorbide dinitrate [47] were also effective in enhancing drug delivery in mouse tumor (Fig. 4) (cf. ref. [46]). Nitroglycerin was found also effective when combined with conventional LMW anticancer drugs in clinical setting [70–73].

Augmentation of drug delivery by using an ACE inhibitor such as enalapril was also demonstrated in vivo in mouse tumors (cf. Fig. 1): the ACE inhibitor, when combined with angiotensin II (AT-II)-induced hypertension, enhanced monoclonal antibody (A-7 directed to gastric cancer)-delivery to about 2-fold [42,74]. Dr. Felix Kratz of Freiburg, Germany,

confirmed a similar effect in a different mouse tumor (personal communication).

AT-II-induced hypertension also facilitated drug delivery to other tumor tissues, as shown in animal tumor models [63,75] as well as in patients with advanced or difficult-to-cure cancers (cf. refs. [42,69]). Blood flow dynamics in tumor tissues are quite different from those in normal tissues or organs. That is, no homeostasis of tumor blood flow volume occurs in tumor tissues: when one induced higher blood pressure by infusing AT-II, tumor blood flow volume, as well as tumor drug delivery, increased progressively [63,64,69,75]. Fig. 6 illustrates vascular permeability under AT-II-induced hypertension: in tumors (B), vascular diameters in tumor will dilate, with widened endothelial cell–cell gaps, thus facilitating more drug leakage; whereas in normal blood vessels (A), blood vessels will constrict, endothelial cell–cell junctions will tighten, and less drug leakage will occur, the result being fewer side effects such as bone marrow suppression and gastrointestinal side effects (see Fig. 6) [17,22,63,69,75].

In clinical settings, many cancer drugs are administered at or near the maximum tolerable dose, so a 2- to 3-fold increase in tumor-selective drug delivery would indeed provide great therapeutic benefits [42,68,69,73]. Clinical application of AT-II-induced hypertension during arterial infusion of SMANCS/Lipiodol to patients with difficult-to-cure cancers such as metastatic liver cancer and cancers of the gallbladder, pancreas, and kidney produced very good responses: drug delivery was greatly enhanced, and the time to regression of tumor mass to 50% of the original size became much shortened [69]. In contrast to these favorable results with the arterial infusion of macromolecular drugs such as SMANCS/Lipiodol and AT-II-induced hypertension, the beneficial effect of arterial infusion of conventional LMW drugs is minimal, if not none, due to very rapid diffusion and no drug retention.

Table 4
Surface charge affecting plasma residence times of different nanoparticles in mice [56,57].^a

| Type of nanoparticle | ζ potential (mV) | Mean particle size (nm) | Plasma residence time | | Remarks |
|--|------------------|-------------------------|-----------------------|-------------------|--|
| | | | T _{1/2} | T _{1/10} | |
| <i>Liposome</i> ⁵⁶ | | | | | |
| Non-PEGylated | –7.31 | 124 | 9.08 h | >24 h | Doxorubicin loaded, DPPC:Chol ^a = 1:1 |
| Weakly cationic | +5.58 | 131 | 4.51 h | 15 h (mean) | Doxorubicin loaded, DPPC:Chol:DC-Chol = 5:4:1, slightly positive |
| Strongly cationic | +24.25 | 95 | <30 min | <10 min | Doxorubicin loaded, DPPC:DC-Chol = 5:5, strongly positive |
| <i>PEG-Polylactate nanoparticles</i> ⁵⁷ | | | | | |
| Weakly anionic | –7.6 | 90–100 | 33.8 min | – | PEG chains are on the surface |
| Strongly anionic | –25.3 | 90–100 | 15 min | – | |
| Strongly anionic | –38.7 | 90–100 | 6 min | – | |
| <i>Chitosan nanoparticle</i> ⁵⁷ | | | | | |
| Weakly anionic | –13.2 | 149.2 | – | 12 h (mean) | CM/MM = 1:2, slightly negative |
| Strongly anionic | –38.4 | 156.0 | – | 3 h (mean) | CM/MM = 2:1, strongly negative |
| Weakly cationic | +14.8 | 150.1 | – | <1 h | CH/MM = 1:1, slightly positive |
| Strongly cationic | +34.6 | 152.7 | – | <1 h | CH/MM = 2:1, strongly positive |

Data modified from refs. [56] and [57].

^a DPPC, dipalmitoylphosphatidylcholine; Chol, cholesterol; CM, carboxymethyl chitosan; MM, methyl methacrylate polymer.

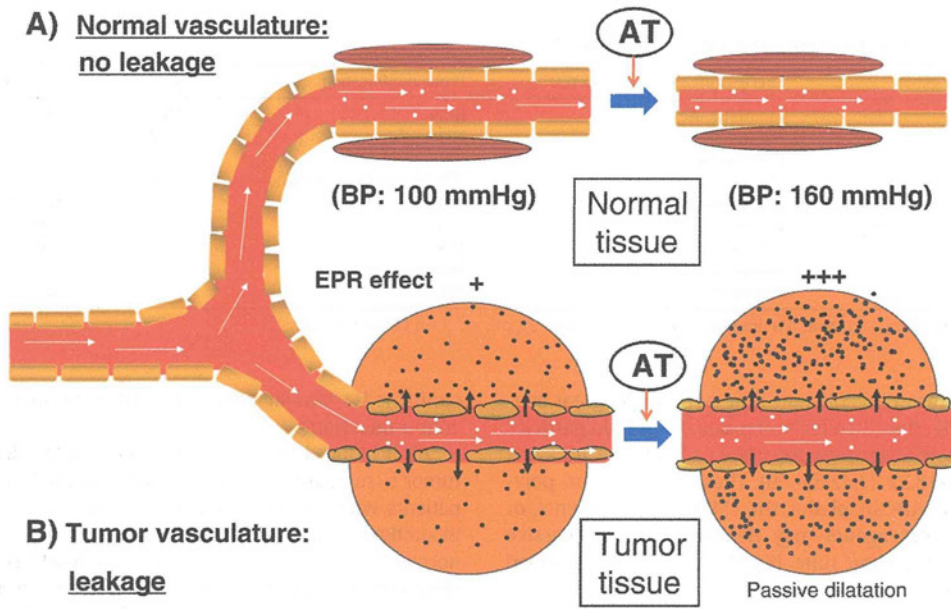


Fig. 6. Diagrammatic representation of the EPR effect and the effect of AT-II-induced hypertension accompanying the enhanced EPR effect and drug delivery in tumor and normal tissue. Under AT-II-induced hypertension (e.g. 100→160 mmHg), normal vessels and tumor vessels behaved differently. (A) The normal blood vessels have a smooth muscle cell layer that contracts and tightens the cell–cell junctions, and a narrowing of the vascular diameter results in less drug leakage. In tumors (B), the vascular endothelial cell–cell junctions have a wide gap opening that will be opened further by elevating blood pressure hydrodynamically (B, right). AT-II-induced hypertension thus leads to enhanced tumor-selective delivery of macromolecular drugs due to gap opening as demonstrated in clinical settings [68]. Adapted from refs. [18] and [68].

All these above vascular mediators are completely safe for almost all patients, and thus we encourage clinicians to validate this strategy. More recently, heme oxygenase-1 (HO-1)/carbon monoxide (CO) [76], TGF- β inhibitor [77], TNF- α [78] and heat generated by laser (He/Ne) together with gold nanorod [36] are shown to augment the EPR effect in mouse models.

6. Fluorescence imaging and the EPR effect with fluorescent nanoprobes

For our initial observation of the EPR effect (in vivo), we used Evans blue, which we administered by intravenous (i.v.) injection, and the tumor was selectively stained blue [16,19,22,23,42], which we

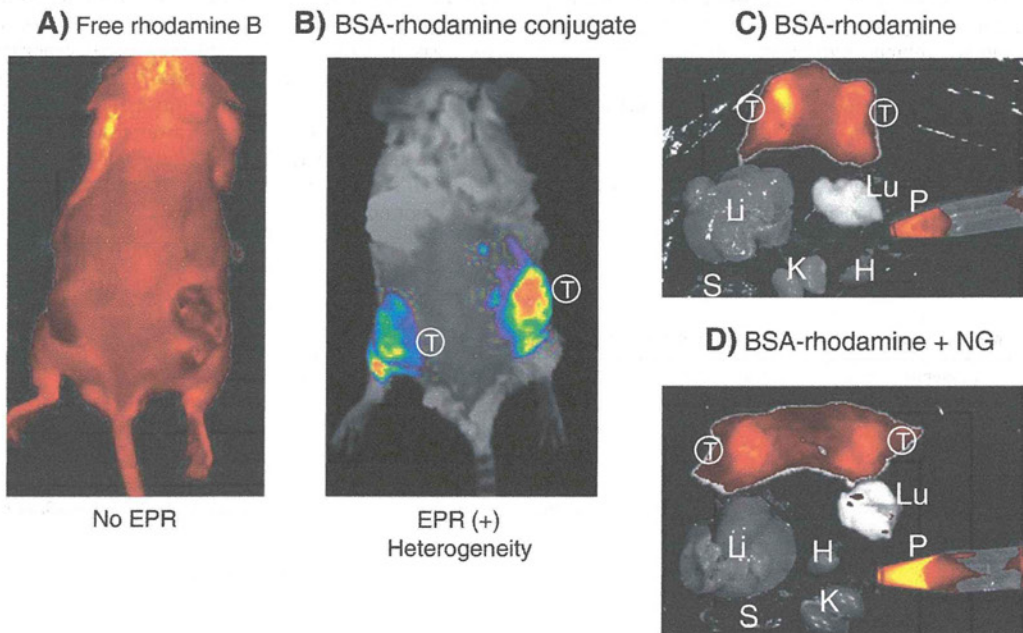


Fig. 7. Fluorescence tumor imaging based on EPR effect. The EPR effect-based uptake of fluorescent nanoprobes in tumors is compared with uptake of parental LMW fluorescent probe in vivo. (A) 24 h after i.v. injection of the LMW fluorescent probe, rhodamine B into S-180 tumor-bearing mice, no distinct tumor image is visible. Whereas injection of tetraethyl rhodamine isothiocyanate (TRITC)-conjugated BSA (67 kDa) resulting in highly tumor selective fluorescence at the same experimental conditions. (C) At 24 h, S-180 tumor-bearing mice were dissected, and each organ was viewed with IVIS® system. Only tumor tissues showed significant fluorescence. (D) Same as C except that nitroglycerin (NG) ointment was applied to the skin, and then the EPR effect and tumor drug delivery were evaluated. In D, the cut surface of tumor tissues shows a more homogeneous fluorescence, and also more fluorescent drug remained in the blood, which indicates that the EPR effect would increase progressively with time. In C and D, fluorescence is not seen in all other normal organs. T, tumor; Li, liver; K, kidney; H, heart; S, spleen; Lu, lung; P, plasma.

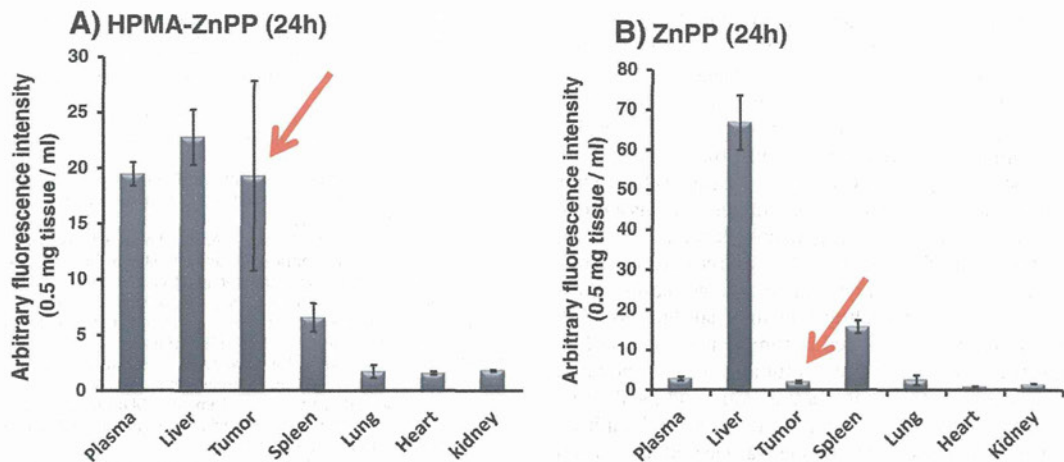
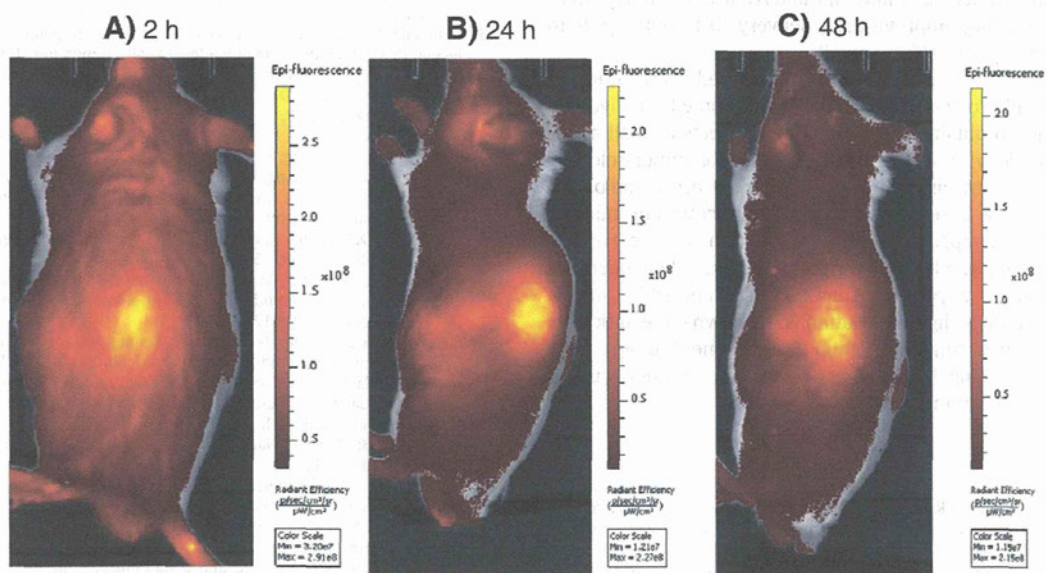


Fig. 8. Tumor selective accumulation of HPMA-conjugate zinc protoporphyrin (HPMA-ZnPP). The specimens were obtained 24 h after iv injection of this conjugate, and fluorescence intensity of each homogenate was measured after extraction of ZnPP with dimethylsulfoxide. Arrows show a great difference in tumor accumulation between (B) free ZnPP vs (A) polymer HPMA conjugated ZnPP.

attributed to the accumulation of blue dye-bound albumin in the tumor. In subsequent studies, we measured various radiolabeled plasma proteins conjugated with radioactive ^{56}Ga via diethylenetriaminepentaacetic acid (DTPA) chelation in solid tumors [16]. Plasma proteins are the most biocompatible macromolecules, and we found that all accumulated in solid tumors more preferentially [16,19,42].

Similarly, when we injected fluorescent macromolecules, we observed tumor-selective staining even 72 hr after i.v. injection. That is, after an i.v. injection of rhodamine isothiocyanate-conjugated bovine serum albumin (BSA) into tumor-bearing mice, we easily and clearly visualized the tumors directly in vivo by using an IVIS imaging system (IVIS, Model Lumina-XR, Hopkinton, MA, a fluorescence imaging system). Fig. 7 illustrates the great difference between tumor imaging obtained with tetramethylrhodamine isothiocyanate (TRITC)-conjugated

BSA [MW 67,000] (Fig. 7B) and that obtained with free rhodamine B (MW 479.1) (Fig. 7A), after i.v. injection into tumor-bearing mice. In contrast to TRITC-BSA, free rhodamine B did not produce any appreciable fluorescence of the tumor (Fig. 7A). This finding clearly demonstrates that the EPR effect also operates for macromolecular fluorescent nanoprobe. We found the same result with another polymer, *N*-(2-hydroxypropyl)methacrylamide (HPMA) (13 kDa) conjugated with zinc protoporphyrin (ZnPP); this conjugate formed micelles of about 80 nm in diameter and showed a clear tumor image similar to Fig. 7B (not shown). To validate accumulation of this fluorescent probe more quantitative manner, we extracted HMPA-ZnPP and measured fluorescence intensity after homogenization of each organ and tumor as well as blood plasma. Fig. 8 illustrates that intra-tumor accumulation at 24 h after iv infusion was more than 10 times of other



The drug is cleared from the normal tissue
 → becoming high S/N by EPR effect

Fig. 9. In vivo tumor imaging by use of indocyanine green (ICG). ICG was injected i.v. into S-180 tumor-bearing mice and in vivo fluorescent imaging was viewed after 2, 24, and 48 h by IVIS system directly. ICG will bind with albumin to form complex, thus behaving as a macromolecule. As shown in the figures, the contrast of the fluorescent tumor image increased as time passes. That is, nonspecific delivery of the agent to normal tissues was cleared via the lymphatic system and thus improving the contrast of tumor image (cf. 2 h vs 48 h).

vital organ such as the heart, lung, kidney except that in the liver that is the major organ for ZnPP metabolism. Since HPMA-ZnPP generates singlet oxygen upon irradiation, endoscopic light irradiation resulted significant tumor suppression in this mouse model (S-180 tumor) (data not shown). Similarly, TRITC-conjugated transferrin also revealed tumor-selective accumulation *in vivo* and a distinct tumor image.

In addition, indocyanine green (ICG) showed clear visible tumor image even 2 h after injection (Fig. 9). ICG is routinely used as a probe for evaluating hepatic function. In healthy people, ICG binds albumin and globulin, and it is rapidly liberated in the liver as free dye, which traverses to the bile duct, and excreted into the bile. Rapid plasma clearance of ICG therefore occurs in healthy humans (half-life < 20 min). Albumin bound ICG rapidly accumulated in tumor, as early as at 2 h, and time-dependent increase of contrast in tumor image is shown in this model (Fig. 9), which is not seen in normal tissue, and the fluorescence of the normal tissues gradually disappeared because of lymphatic clearance. Namely, the fluorescent nanoprobe was cleared faster from the normal tissue than from the tumor tissue, and thus the contrast of the tumor image improved progressively after 24 and then 48 h. This finding confirms the distinct retention of fluorescent nanoprobe in tumors based on the EPR effect (Figs. 7–9). It is therefore so obvious that radio emitting nuclei or positron emitting or magnetic resonance probes in biocompatible nanoparticles would have a great value similarly for tumor imaging and an important value to offer.

7. Conclusions

Our history of the discovery of EPR effect is briefly reviewed. Comparison of the vascular permeability of tumor tissues as well as inflamed tissue illustrate the relevance of the EPR effect for cancer treatment and diagnosis. Many vascular factors such as bradykinin, NO, prostaglandin and CO were shown to be produced excessively in both inflammation and cancer, and modulation of these factors may potentiate the EPR effect. The defective architecture of tumor vessels and the vascular factors affecting normal tissue surrounding tumors also contribute to macromolecular permeability of the EPR effect as well.

Methods to enhance the EPR effect that utilize nitroglycerin and other NO-releasing agents, ACE inhibitors, and AT-II-induced hypertension, among others, may improve drug delivery to tumors by 2- to 3-fold and thus therapeutic effect as well.

We expect that the use of polymers or nanomedicines to deliver drugs to tumors will provide great advantages not only for delivery of therapeutic agents to obtain better therapeutic effects as well as reduced systemic toxicity; it will be invaluable also for tumor-selective and highly sensitive imaging with fluorescent or other radiological nanoprobe. Providing detection methods for microtumor nodules would make earlier therapeutic surgical intervention possible. Further, a similar method is applicable for using photosensitizer of nanoparticle, which generates singlet oxygen and tumor detection possible simultaneously under endoscopic light irradiation (not shown). We anticipate a great advancement in tumor detection and treatment at very early stage of tumor before long, by use of nanomedicine, and more cure of cancer would be achieved in one way or the other.

References

- [1] K. Matsumoto, T. Yamamoto, R. Kamata, H. Maeda, Pathogenesis of serratal infection: activation of the Hageman factor-prekallikrein cascade by serratal protease, *J. Biochem.* 96 (1984) 739–749.
- [2] R. Kamata, T. Yamamoto, K. Matsumoto, H. Maeda, A serratal protease causes vascular permeability reaction by activation of the Hageman factor-dependent pathway in guinea pigs, *Infect. Immun.* 48 (1985) 747–753.
- [3] A. Molla, T. Yamamoto, T. Akaike, S. Miyoshi, H. Maeda, Activation of Hageman factor and prekallikrein and generation of kinin by various microbial proteinases, *J. Biol. Chem.* 264 (1989) 10589–10594.
- [4] K. Maruo, T. Akaike, Y. Inada, I. Ohkubo, T. Ono, H. Maeda, Effect of microbial and mite proteases on low and high molecular weight kininogens, *J. Biol. Chem.* 268 (1993) 17711–17715.
- [5] H. Maeda, T. Yamamoto, Pathogenic mechanisms induced by microbial proteases in microbial infections, *Biol. Chem.* 377 (1996) 217–226.
- [6] H. Maeda, Y. Matsumura, H. Kato, Purification and identification of [hydroxypropyl³] bradykinin in ascitic fluid from a patient with gastric cancer, *J. Biol. Chem.* 263 (1988) 16051–16054.
- [7] Y. Matsumura, M. Kimura, T. Yamamoto, H. Maeda, Involvement of the kinin-generating cascade and enhanced vascular permeability in tumor tissue, *Jpn. J. Cancer Res.* 79 (1988) 1327–1334.
- [8] Y. Matsumura, K. Maruo, M. Kimura, T. Yamamoto, T. Konno, H. Maeda, Kinin-generating cascade in advanced cancer patients and *in vitro* study, *Jpn. J. Cancer Res.* 82 (1991) 732–741.
- [9] H. Maeda, Y. Noguchi, K. Sato, T. Akaike, Enhanced vascular permeability in solid tumor is mediated by nitric oxide and inhibited by both new nitric oxide scavenger and nitric oxide synthase inhibitor, *Jpn. J. Cancer Res.* 85 (1994) 331–334.
- [10] K. Doi, T. Akaike, H. Horie, Y. Noguchi, S. Fujii, T. Beppu, M. Ogawa, H. Maeda, Excessive production of nitric oxide in rat solid tumor and its implication in rapid tumor growth, *Cancer* 77 (1996) 1598–1604.
- [11] H. Maeda, T. Akaike, J. Wu, Y. Noguchi, Y. Sakata, Bradykinin and nitric oxide in infectious disease and cancer, *Immunopharmacology* 33 (1996) 222–230.
- [12] J. Wu, T. Akaike, K. Hayashida, T. Okamoto, A. Okuyama, H. Maeda, Enhanced vascular permeability in solid tumor involving peroxynitrite and matrix metalloproteinase, *Jpn. J. Cancer Res.* 92 (2001) 439–451.
- [13] J. Wu, T. Akaike, H. Maeda, Modulation of enhanced vascular permeability in tumors by a bradykinin antagonist, a cyclooxygenase inhibitor, and a nitric oxide scavenger, *Cancer Res.* 58 (1998) 159–165.
- [14] S. Tanaka, T. Akaike, S.J. Wu, J. Fang, T. Sawa, M. Ogawa, T. Beppu, H. Maeda, Modulation of tumor-selective vascular blood flow and extravasation by the stable prostaglandin I₂ analogue beraprost sodium, *J. Drug Target.* 11 (2003) 45–52.
- [15] H. Maeda, J. Fang, T. Inuzuka, Y. Kitamoto, Vascular permeability enhancement in solid tumor: various factors, mechanisms involved and its implications, *Int. Immunopharmacol.* 3 (2003) 319–328.
- [16] Y. Matsumura, H. Maeda, A new concept for macromolecular therapeutics in cancer chemotherapy: mechanism of tumorotropic accumulation of proteins and the antitumor agent SMANCS, *Cancer Res.* 46 (1986) 6387–6392.
- [17] H. Maeda, The enhanced permeability and retention (EPR) effect in tumor vasculature: the key role of tumor-selective macromolecular drug targeting, in: G. Weber (Ed.), *Advances in Enzyme Regulation*, Elsevier Science Ltd., Oxford, 2001, pp. 189–207.
- [18] H. Maeda, Tumor-selective delivery of macromolecular drugs via the EPR effect: background and future prospects, *Bioconjug. Chem.* 21 (2010) 797–802.
- [19] J. Fang, H. Nakamura, H. Maeda, The EPR effect: unique features of tumor blood vessels for drug delivery, factors involved, and limitations and augmentation of the effect, *Adv. Drug Deliv. Rev.* 63 (2011) 136–151.
- [20] Y. Noguchi, J. Wu, R. Duncan, J. Strohal, K. Ulbrich, T. Akaike, H. Maeda, Early phase tumor accumulation of macromolecules: a great difference in clearance rate between tumor and normal tissues, *Jpn. J. Cancer Res.* 89 (1998) 307–314.
- [21] L.W. Seymour, Y. Miyamoto, H. Maeda, M. Brereton, J. Strohal, K. Ulbrich, R. Duncan, Influence of molecular weight on passive tumour accumulation of a soluble macromolecular drug carrier, *Eur. J. Cancer* 31 (1995) 766–770.
- [22] H. Maeda, J. Wu, T. Sawa, Y. Matsumura, K. Hori, Tumor vascular permeability and the EPR effect in macromolecular therapeutics, *J. Control. Release* 65 (2000) 271–284.
- [23] H. Maeda, T. Sawa, T. Konno, Mechanism of tumor-targeted delivery of macromolecular drugs, including the EPR effect in solid tumor and clinical overview of the prototype polymeric drug SMANCS, *J. Control. Release* 74 (2001) 47–61.
- [24] T.M. Allen, P.R. Cullis, Drug delivery systems: entering the mainstream, *Science* 303 (2004) 1818–1822.
- [25] T. Nam, S. Park, S.Y. Lee, K. Park, K. Choi, I.C. Song, M.H. Han, J.J. Leary, S.A. Yuk, I.C. Kwon, K. Kim, S.Y. Jeong, Tumor targeting chitosan nanoparticles for dual-modality optical/MR cancer imaging, *Bioconjug. Chem.* 21 (2010) 578–582.
- [26] M. Silindir, S. Erdoğan, A.Y. Özer, S. Maia, Liposomes and their applications in molecular imaging, *J. Drug Target.* 20 (2012) 401–415.
- [27] A. Mahmud, X.B. Xiong, H.M. Aliabadi, A. Lavasanifar, Polymeric micelles for drug targeting, *J. Drug Target.* 15 (2007) 553–584.
- [28] K. Jakobsohn, M. Motiei, M. Sinvani, R. Popovtzer, Towards real-time detection of tumor margins using photothermal imaging of immune-targeted gold nanoparticles, *Int. J. Nanomedicine* 7 (2012) 4707–4713.
- [29] P. Pellegrin, A. Fernandez, N.J.C. Lamb, R. Bennes, Macromolecular uptake is a spontaneous event during mitosis in cultured fibroblasts: implications for vector-dependent plasmid transfection, *Mol. Biol. Cell* 13 (2002) 570–578.
- [30] S.D. Li, L. Huang, Pharmacokinetics and biodistribution of nanoparticles, *Mol. Pharm.* 5 (2008) 496–504.
- [31] R. Duncan, R. Gaspar, Nanomedicine(s) under the microscope, *Mol. Pharm.* 8 (2011) 2101–2141.
- [32] S.M. Moghimi, A.C. Hunter, J.C. Murray, Nanomedicine: current status and future prospects, *FASEB J.* 19 (2005) 311–330.
- [33] M. Ogawa, C.A. Regino, J. Seidel, M.V. Green, W. Xi, M. Williams, N. Kosaka, P.L. Choyke, H. Kobayashi, Dual-modality molecular imaging using antibodies labeled with activatable fluorescence and a radionuclide for specific and quantitative targeted cancer detection, *Bioconjug. Chem.* 20 (2009) 2177–2184.
- [34] S. Keereweer, I.M. Mol, J.D. Kerrebijn, P.B. Van Driel, B. Xie, R.J.B. Jong, A.L. Vahrmeijer, C.W. Löwik, Targeting integrins and enhanced permeability and retention (EPR) effect for optical imaging of oral cancer, *J. Surg. Oncol.* 105 (2012) 714–718.
- [35] F. Yu, L. Zhang, Y. Huang, K. Sun, A.E. David, V.C. Yanga, The magnetophoretic mobility and superparamagnetism of core-shell iron oxide nanoparticles with dual targeting and imaging functionality, *Biomaterials* 31 (2010) 5842–5848.

- [36] A.J. Gormley, N. Larson, S. Sadekar, R. Robinson, A. Ray, H. Ghandehari, Guided delivery of polymer therapeutics using plasmonic photothermal therapy, *Nano Today* 7 (2012) 158–167.
- [37] In: F. Kratz, P. Senter, H. Steinhagen (Eds.), *Drug Delivery in Oncology, From Basic Research to Cancer Therapy*, vol. 1–3, Wiley-VCH Verlag GmbH & Co. KG, Weinheim, Germany, 2011, pp. 1–1689.
- [38] D.R. Senger, S.J. Galli, A.M. Dvorak, C.A. Perruzzi, V.S. Harvey, H.F. Dvorak, Tumor cells secrete a vascular permeability factor that promotes accumulation of ascites fluid, *Science* 219 (1983) 983–985.
- [39] H.F. Dvorak, J.A. Nagy, J.T. Dvorak, A.M. Dvorak, Identification and characterization of the blood vessels of solid tumors that are leaky to circulating macromolecules, *Am. J. Pathol.* 133 (1988) 95–109.
- [40] J. Folkman, Tumor angiogenesis: therapeutic implications, *N. Engl. J. Med.* 285 (1971) 1182–1186.
- [41] J. Folkman, What is the evidence that tumors are angiogenesis dependent? *J. Natl. Cancer Inst.* 82 (1990) 4–6.
- [42] H. Maeda, Vascular permeability in cancer and infection as related to macromolecular drug delivery, with emphasis on the EPR effect for tumor-selective drug targeting, *Proc. Jpn. Acad. B Phys. Biol. Sci.* 88 (2012) 53–71.
- [43] T. Akaike, Y. Noguchi, S. Ijiri, K. Setoguchi, M. Suga, Y.M. Zheng, B. Dietzschold, H. Maeda, Pathogenesis of influenza virus-induced pneumonia: involvement of both nitric oxide and oxygen radicals, *Proc. Natl. Acad. Sci. U. S. A.* 93 (1996) 2448–2453.
- [44] T. Oda, T. Akaike, T. Hamamoto, F. Suzuki, T. Hirano, H. Maeda, Oxygen radicals in influenza-induced pathogenesis and treatment with pyran polymer-conjugated SOD, *Science* 244 (1989) 974–976.
- [45] H. Maeda, T. Akaike, Oxygen free radicals as pathogenic molecules in viral diseases, *Proc. Soc. Exp. Biol. Med.* 198 (1991) 721–727.
- [46] T. Seki, J. Fang, H. Maeda, Enhanced delivery of macromolecular antitumor drugs to tumors by nitroglycerin application, *Cancer Sci.* 100 (2009) 2426–2430.
- [47] H. Maeda, Nitroglycerin enhances vascular blood flow and drug delivery in hypoxic tumor tissues: analogy between angina pectoris and solid tumors and enhancement of the EPR effect, *J. Control. Release* 142 (2010) 296–298.
- [48] A. Matsuzawa, H. Ichijo, Redox control of cell fate by MAP kinase: physiological roles of ASK1-MAP kinase pathway in stress signaling, *Biochim. Biophys. Acta* 1780 (2008) 1325–1336.
- [49] K. Shiratori, X. Jin, I. Ilieva, Y. Koyama, K. Yazawa, K. Yoshida, S. Kase, S. Ohno, Suppressive effects of astaxanthin against rat endotoxin-induced uveitis by inhibiting the NF- κ B signaling pathway, *Exp. Eye Res.* 82 (2006) 275–281.
- [50] M. Wlaschek, G. Heinen, A. Poswig, A. Schwarz, T. Krieg, K. Scharfetter-Kochanek, UVA-induced autocrine stimulation of fibroblast-derived collagenase/MMP-1 by interrelated loops of interleukin-1 and interleukin-6, *Photochem. Photobiol.* 59 (1994) 550–556.
- [51] I. Kramarenko, T. Morinelli, M. Bunn, J. Raymond Sr., M. Garnovskaya, The bradykinin B₂ receptor induces multiple cellular responses leading to the proliferation of human renal carcinoma cell lines, *Cancer Treat. Res.* 4 (2012) 195–205.
- [52] X. Cao, T. Tsukamoto, T. Seki, H. Tanaka, S. Morimura, L. Cao, T. Mizoshita, H. Ban, T. Toyoda, H. Maeda, M. Tatematsu, 4-Vinyl-2,6-dimethoxyphenol (canolol) suppresses oxidative stress and gastric carcinogenesis in *Helicobacter pylori*-infected carcinogen-treated Mongolian gerbils, *Int. J. Cancer* 122 (2008) 1445–1454.
- [53] H. Maeda, Y. Matsumura, T. Oda, K. Sasamoto, Cancer selective macromolecular therapeutics: tailoring of an antitumor protein drug, in: R.E. Feeney, J.R. Whitaker (Eds.), *Protein Tailoring for Food and Medical Uses*, Marcel Dekker, New York, 1986, pp. 353–382.
- [54] H. Maeda, T. Matsumoto, T. Konno, K. Iwai, M. Ueda, Tailor-making of protein drugs by polymer conjugation for tumor targeting: a brief review on smancs, *J. Protein Chem.* 3 (1984) 181–193.
- [55] H. Maeda, Polymer conjugated macromolecular drugs for tumor-specific targeting, in: A.J. Domb (Ed.), *Polymeric Site-Specific Pharmacotherapy*, John Wiley & Sons, New York, 1994, pp. 95–116.
- [56] C. He, Y. Hu, L. Yin, C. Tang, C. Yin, Effects of particle size and surface charge on cellular uptake and biodistribution of polymeric nanoparticles, *Biomaterials* 31 (2010) 3657–3666.
- [57] J.S. Lee, M. Ankone, E. Pieters, R.M. Schifferers, W.E. Hennink, J. Feijen, Circulation kinetics and biodistribution of dual-labeled polymersomes with modulated surface charge in tumor-bearing mice: comparison with stealth liposomes, *J. Control. Release* 155 (2011) 282–288.
- [58a] T. Oda, T. Morinaga, H. Maeda, Stimulation of macrophage by polyanions and its conjugated proteins and effect on cell membrane, *Proc. Soc. Exp. Biol. Med.* 181 (1986) 9–17.
- [58b] T. Oda, H. Maeda, Binding to and internalization by cultured cells of neocarzinostatin and enhancement of its actions by conjugation with lipophilic styrene-maleic acid copolymer, *Cancer Res.* 47 (1987) 3206–3211.
- [58c] T. Oda, F. Sato, H. Maeda, Facilitated internalization of neocarzinostatin and its lipophilic polymer conjugate, SMANCS, into cytosol in acidic pH, *J. Nat. Cancer Inst.* 9 (1987) 1205–1211.
- [58d] H. Nakamura, J. Fang, B. Gahinath, K. Tsukigawa, H. Maeda, Intracellular uptake and behavior of two types zinc protoporphyrin (ZnPP) micelles, SMA-ZnPP and PEG-ZnPP as anticancer agents; Unique intracellular disintegration of SMA micelles, *J. Control. Release* 155 (2011) 367–375.
- [58e] T. Oda, Y. Kojima, T. Akaike, S. Ijiri, A. Molla, H. Maeda, Inactivation of chemotactic activity of C5a by the serratal 56-kilodalton protease, *Infect. Immun.* 58 (1990) 1269–1272.
- [59] H. Maeda, M. Ueda, T. Morinaga, T. Matsumoto, Conjugation of poly (styrene-co-maleic acid) derivatives to the antitumor protein neocarzinostatin: pronounced improvements in pharmacological properties, *J. Med. Chem.* 28 (1985) 455–461.
- [60] S. Skinner, P. Tutton, P. O'Brien, Microvascular architecture of experimental colon tumors in the rat, *Cancer Res.* 50 (1990) 2411–2417.
- [61] M.A. Konerding, A.J. Miodonski, A. Lametschwandner, Microvascular corrosion casting in the study of tumor vascularity: a review, *Scanning Microsc.* 9 (1995) 1233–1244.
- [62] H. Hashizume, P. Baluk, S. Morikawa, J.W. McLean, G. Thurston, S. Roberge, R.K. Jain, D.M. McDonald, Openings between defective endothelial cells explain tumor vessel leakiness, *Am. J. Pathol.* 1561 (2000) 1363–1380.
- [63] M. Suzuki, K. Hori, I. Abe, S. Saito, H. Sato, A new approach to cancer chemotherapy: selective enhancement of tumor blood flow with angiotensin II, *J. Natl. Cancer Inst.* 67 (1981) 663–669.
- [64] K. Hori, S. Saito, H. Takahashi, H. Sato, H. Maeda, Y. Sato Tumor-selective, blood flow decrease induced by an angiotensin converting enzyme inhibitor, temocapril hydrochloride, *Jpn. J. Cancer Res.* 91 (2000) 261–269.
- [65] K. Iwai, H. Maeda, T. Konno, Use of oily contrast medium for selective drug targeting to tumor: enhanced therapeutic effect and X-ray image, *Cancer Res.* 44 (1984) 2115–2121.
- [66] T. Konno, H. Maeda, K. Iwai, S. Maki, S. Tashiro, M. Uchida, Y. Miyauchi, Selective targeting of anticancer drug and simultaneous image enhancement in solid tumors by arterially administered lipid contrast medium, *Cancer* 54 (1984) 2367–2374.
- [67] S. Maki, T. Konno, H. Maeda, Image enhancement in computerized tomography for sensitive diagnosis of liver cancer and semiquantitation of tumor selective drug targeting with oily contrast medium, *Cancer* 56 (1985) 751–757.
- [68] T. Konno, H. Maeda, K. Iwai, S. Tashiro, S. Maki, T. Morinaga, M. Mochinaga, M.T. Hiraoka, I. Yokoyama, Effect of arterial administration of high-molecular-weight anticancer agent SMANCS with lipid lymphographic agent on hepatoma: a preliminary report, *Eur. J. Cancer Clin. Oncol.* 19 (1983) 1053–1065.
- [69] A. Nagamitsu, K. Greish, H. Maeda, Elevating blood pressure as a strategy to increase tumor targeted delivery of macromolecular drug SMANCS: cases of advanced solid tumors, *Jpn. J. Clin. Oncol.* 39 (2009) 756–766.
- [70] H. Yasuda, M. Yamaya, K. Nakayama, T. Sasaki, S. Ebihara, A. Kanda, M. Asada, D. Inoue, T. Suzuki, T. Okazaki, H. Takahashi, M. Yoshida, T. Kaneta, K. Ishizawa, S. Yamanda, N. Tomita, M. Yamasaki, A. Kikuchi, H. Kubo, H. Sasaki, Randomized phase II trial comparing nitroglycerin plus vinorelbine and cisplatin with vinorelbine and cisplatin alone in previously untreated stage IIIB/IV non-small cell lung cancer, *J. Clin. Oncol.* 24 (2006) 688–694.
- [71] H. Yasuda, K. Nakayama, M. Watanabe, S. Suzuki, H. Fujii, S. Okinaga, A. Kanda, K. Zayazu, T. Sasaki, M. Asada, T. Suzuki, M. Yoshida, S. Yamanda, D. Inoue, T. Kaneta, T. Kondo, Y. Takai, H. Sasaki, K. Yanagihara, M. Yamaya, Nitroglycerin treatment may increase response to docetaxel and carboplatin regimen via inhibitions of hypoxia-inducible factor-1 pathway and P-glycoprotein in patients with lung adenocarcinoma, *Clin. Cancer Res.* 12 (2006) 6748–6757.
- [72] H. Yasuda, K. Yanagihara, K. Nakayama, T. Mio, T. Sasaki, M. Asada, M. Yamaya, M. Fukushima, Therapeutic applications of nitric oxide for malignant tumor in animal models and human studies, in: B. Bonavida (Ed.), *Nitric Oxide and Cancer*, Springer Science, New York, 2010, pp. 419–441.
- [73] D.R. Siemens, J.P.W. Heaton, M.A. Adams, J. Kawakami, C.H. Graham, Phase II study of nitric oxide donor for men with increasing prostate-specific antigen level after surgery or radiotherapy for prostate cancer, *Urology* 74 (2009) 878–883.
- [74] A. Noguchi, T. Takahashi, T. Yamaguchi, K. Kitamura, A. Noguchi, H. Tsurumi, K. Takashina, H. Maeda, Enhanced tumor localization of monoclonal antibody by treatment with kinase II inhibitor and angiotensin II, *Jpn. J. Cancer Res.* 83 (1992) 240–243.
- [75] C.J. Li, Y. Miyamoto, Y. Kojima, H. Maeda, Augmentation of tumour delivery of macromolecular drugs with reduced bone marrow delivery by elevating blood pressure, *Br. J. Cancer* 67 (1993) 975–980 M.R.
- [76] J. Fang, H. Qin, H. Nakamura, K. Tsukigawa, H. Maeda, Carbon monoxide, generated by heme oxygenase-1, mediates the enhanced permeability and retention (EPR) effect of solid tumor, *Cancer Sci.* 102 (2012) 535–541.
- [77] Kano, Y. Bae, C. Iwata, Y. Morishita, M. Yashiro, M. Oka, T. Fujii, A. Komuro, K. Kiyono, M. Kaminishi, K. Hirakawa, Y. Ouchi, N. Nishiyama, K. Kataoka, K. Miyazono, Improvement of cancer-targeting therapy, using nanocarriers for intractable solid tumors by inhibition of TGF- β signaling, *Proc. Natl. Acad. Sci. U. S. A.* 104 (2007) 3460–3465.
- [78] T. Seki, F. Carroll, S. Illingworth, N. Green, R. Cawood, H. Bachtarzi, V. Subr, K.D. Fisher, L.W. Seymour, Tumour necrosis factor- α increases extravasation of virus particles into tumour tissue by activating the Rho A/Rho kinase pathway, *J. Control. Release* 156 (2011) 381–389.

Meeting Report

Challenges and Key Considerations of the Enhanced Permeability and Retention Effect for Nanomedicine Drug Delivery in Oncology

Uma Prabhakar¹, Hiroshi Maeda², Rakesh K. Jain³, Eva M. Sevick-Muraca⁵, William Zamboni⁶, Omid C. Farokhzad⁴, Simon T. Barry⁷, Alberto Gabizon⁸, Piotr Grodzinski¹, and David C. Blakey⁷

Abstract

Enhanced permeability of the tumor vasculature allows macromolecules to enter the tumor interstitial space, whereas the suppressed lymphatic filtration allows them to stay there. This phenomenon, enhanced permeability and retention (EPR), has been the basis of nanotechnology platforms to deliver drugs to tumors. However, progress in developing effective drugs using this approach has been hampered by heterogeneity of EPR effect in different tumors and limited experimental data from patients on effectiveness of this mechanism as related to enhanced drug accumulation. This report summarizes the workshop discussions on key issues of the EPR effect and major gaps that need to be addressed to effectively advance nanoparticle-based drug delivery. *Cancer Res*; 73(8): 2412–7. ©2013 AACR.

Introduction

The field of nanomedicine, despite being conceptualized as far back as the 1980s, is only now transitioning in a broad sense from academic research to drug development and commercialization. In oncology, unique structural features of many solid tumors, including hypervascularity, defective vascular architecture, and impaired lymphatic drainage leading to the well-characterized enhanced permeability and retention (EPR; ref. 1) effect, are key factors in advancing this platform technology. However, the EPR effect has been measured mostly, if not exclusively, in implanted tumors with limited data on EPR in metastatic lesions. Dextran-coated iron oxide nanoparticles (25–50 nm) have been used clinically for several years (2) to measure permeability and retention noninvasively by MRI (3). Furthermore, tumor response alone is no longer considered a good endpoint, at least from the health authority point of

view. This is exemplified by the recent U.S. Food and Drug Administration (FDA) withdrawal of bevacizumab (Avastin) for patients with metastatic breast cancer where impressive tumor responses were seen but bevacizumab showed no improvement in overall survival. Thus, limitations and challenges both in understanding tumor structural features and correlating them with the technology must be addressed and additional critical data need to be generated before nanotechnology-based drug delivery approaches can be fully realized in clinical use in patients with cancer. A one-day workshop was convened at the NIH on October 10, 2012, to specifically address key issues related to understanding of EPR effect and its use to achieve the maximum therapeutic effect with drugs using nanoparticle carriers.

This workshop was organized by the Alliance for Nanotechnology in Cancer and its recently formed public–private partnership consortium, TONIC (Translation of Nanotechnology in Cancer), in response to several questions raised by industry members of TONIC. The main purpose of this meeting was to gain better understanding of the EPR characteristics impacting the use of nanoparticles in the clinic. Experimental evidence of EPR in animal models and humans, clinical relevance of EPR, gaps in knowledge, and ways to address these gaps were all discussed.

Report

The workshop composed of 8 talks covering topics ranging from methods to investigate EPR in preclinical and clinical studies including diagnostic imaging, to the ramifications of EPR for enhanced drug uptake by different tumors and the predictability of preclinical and clinical outcomes. The session opened with an overview of the nanotechnology programs in cancer, funded by the Alliance for Nanotechnology in Cancer (NCI), and was followed by an introduction to TONIC, a corporate partnership model of the public, private, and

Authors' Affiliations: ¹Alliance for Nanotechnology in Cancer, National Cancer Institute, Bethesda, Maryland; ²Institute for DDS Research, Sojo University, Kumamoto, Japan; ³Harvard Medical School and Massachusetts General Hospital; ⁴Harvard Medical School and Brigham and Women's Hospital, Boston, Massachusetts; ⁵Brown Foundation Institute of Molecular Medicine, The University of Texas Health Science Center, Houston, Texas; ⁶UNC Eshelman School of Pharmacy, UNC Lineberger Comprehensive Cancer Center, University of North Carolina, Chapel Hill, North Carolina; ⁷AstraZeneca, Alderley Park, Macclesfield, United Kingdom; and ⁸Shaare Zedek Medical Center and Hebrew University–School of Medicine, Jerusalem, Israel

Note: A list of speakers is available as supplementary data for this article at Cancer Research Online (<http://cancerres.aacrjournals.org/>).

Corresponding Authors: Uma Prabhakar, Office of Cancer Nanotechnology Research, National Cancer Institute, Building 31–Room 10A52, Bethesda, MD 20892. Phone: 267-574-4101; Fax: 301-496-7807; E-mail: uma.prabhakar@nih.gov; and Piotr Grodzinski, E-mail: grodzinp@mail.nih.gov

doi: 10.1158/0008-5472.CAN-12-4561

©2013 American Association for Cancer Research.

academic sectors, to accelerate the translation and development of nanotechnology solutions for the early detection, diagnosis, and treatment of cancer. This was followed by scientific presentations relating to the key questions identified at previous TONIC meetings. The discussions at the workshop focused on two key themes, namely, heterogeneity of EPR in tumors and factors that influence EPR effect.

Heterogeneity of EPR in Tumors

EPR exists in tumors and can be exploited for selective delivery of drugs to tumor by nanotechnology. However, there is significant heterogeneity within and between tumor types. It was noted that different tumor types have different pore dimensions in the vasculature and that the maximum pore size changes with the location for a given type of tumor (i.e., primary vs. metastases). In addition, there may be differences in vessel structure within a single tumor type. Thus, to understand whether a tumor is likely to respond to a nanoparticle-based drug that relies on EPR for delivery, an image-guided patient selection or diagnostic approach can potentially prove useful to profile and select tumor types and patients with tumors conducive to such delivery. Hiroshi Maeda (Sojo University, Kumamoto, Japan), who first proposed the EPR effect over 25 years ago (1), suggested a number of ways one can augment the EPR effect. These included increasing the blood pressure during infusion of a nanomedicine or macromolecular drug using angiotensin-II (e.g., blood pressure increase from 100 → 150 mmHg). Other methods involve vascular mediators such as nitroglycerin, ACE inhibitor, or PGE1 agonist (beraprost) and these have been shown to be effective in *in vivo* tumor models resulting in better tumor delivery (2- to 3-fold increase), linked to improved therapeutic effect (4).

Factors Influencing EPR

The following factors influence the EPR effect in tumors: (i) the nature of both the vascular bed and surrounding stroma, the presence or absence of functional lymphatics and interstitial hydraulic conductivity impacting interstitial pressure along with mechanical stresses generated by cancer and stromal cells impacting the extracellular matrix; (ii) tumor size, type, and location (including primary tumor versus metastatic lesions); (iii) extent of macrophage tumor infiltration and the activity of the mononuclear phagocytic system (MPS), which can vary between and within tumor types plus patient characteristics (e.g., age, gender, tumor type, body composition, treatment). These factors lead to accumulation of nanoparticles in both normal tissues and in different sections of the tumor, for example, in the periphery, viable tumor, and necrotic sections; and (iv) co-medications, which may impact, among other things, stroma and blood pressure (hypertension increases tumor blood flow). In addition, several vascular factors (Table 1; ref. 4), such as nitric oxide generators (5) and bradykinin potentiators, that is, ACE inhibitors that lower blood pressure, are known to affect EPR and are relatively safe and inexpensive to combine with a nanoparticle drug (4).

A fundamental limitation in evaluating EPR and the factors that affect EPR is poor understanding of which preclinical

tumor models recapitulate patients with solid tumors. The factors affecting delivery of nanoparticles to tumors in pre-clinical models, such as tumor growth environment, vasculature, functional MPS, etc., appear to vary based on the cancer model [e.g., syngeneic flank xenograft, orthotopic xenograft, genetically engineered mouse model (GEMM)]. Thus, future studies will need to systemically evaluate these factors in preclinical models and in patients with various solid tumors and determine whether the models represent all aspects of the EPR effect.

The observed heterogeneity in EPR may be a contributing factor to the limited impact of nanoparticle-based drugs with reductions in toxicity and gains in overall survival as compared with small-molecule anti-cancer agents. Table 2 summarizes objective data on the survival benefits from nanotherapeutics approved to date. Further understanding and predictability of EPR function in primary tumor and its metastatic sites through the use of imaging studies may aid the development of future, effective nanodrugs. Correlation of EPR activity to clinical responses would likely provide direct clinical data to determine whether tumors with high EPR tumor activity will be more amenable to effective treatment using nanoparticle-based therapies (5). It was noted that the diversity of nanoparticle characteristics and API used is expected to impact the applicability of such correlations across different nanoparticle platforms and products.

The optimal patient selection or diagnostic aid to measure the EPR activity within a patient needs to be further defined. Ideally, this would involve a single imaging agent that is generalizable to all nanoparticles. Given the heterogeneity of nanoparticle-based systems—size, shape, charge characteristics, etc.—a specific diagnostic agent might, however, be required to predict likely response to a particular nanoparticle relying on EPR delivery. The use of contrast agents and MRI to measure the enhanced permeability (EP) component of the EPR effect might be one generic method. Others might include a defined nanoparticle of a fixed size (~100 nm) labeled with an appropriate imaging agent—for example, Cu⁶⁴ for positron emission tomography (PET) or fluorescent marker for near-infrared fluorescence (NIRF). There is precedence for a range of labeled liposomes and iron oxide-loaded nanoparticles for imaging, but there are very few human clinical studies on nanoparticle imaging that can effectively address the prevalence of EPR. In one such study, the biodistribution and pharmacokinetics of [¹¹¹In]-labeled PEGylated liposomes was evaluated in patients with locally advanced cancers. Positive tumor images were obtained in 15 of 17 studies, although levels of tumor liposome uptake varied between and within tumor types (6).

Eva Sevick-Muraca (The University of Texas Health Science Center, Houston, Texas) discussed the use of NIRF to image lymphatic flow and with fluorescent agents to detect cancers. This technique is light based and the fluorescent dye has no half-life and can be repeatedly excited, making it more appropriate for imaging of nanoparticle accumulation over longer timeframes than radioactive imaging agents with short half-lives (7). While NIRF is considered to be a combination product by the FDA and has a maximum tissue penetration of 3 to 5 cm,

Table 1. Factors affecting the EPR effect of macromolecular drugs in solid tumors (modified after references 4 and 5)

| Mediators | Responsible enzymes and mechanisms | Possible application to therapeutic modality and mechanism |
|---|---|---|
| Bradykinin | Kallikrein/protease | ACE inhibitors (e.g., enalapril); blocking of kinin degradation elevates local kinin level → more EPR. |
| NO | iNOS | NO-releasing agents (e.g., nitroglycerin, ISDN, etc.) via denitrase and nitrite reductase to generate NO. |
| VPF/VEGF Prostaglandins | Involved in NO generation COX-1 | Beraprost sodium: PGI ₂ agonist works via vascular dilatation and extravasation (5). |
| Collagenase (MMP) | Activated from proMMPs by peroxynitrite, or proteases | |
| Peroxyntirite Carbon monoxide (CO) | NO + O ₂ Heme oxygenase (HO)-1 | PEG-hemine via induction of HO-1 in tumor → CO generation (15). |
| Induced hypertension | Using angiotensin II | Slow i.v. infusion → systemic hypertension, vascular extravasation selectively in tumor tissue. |
| Inflammatory cells and H ₂ O ₂ TGF-β inhibitor | Neutrophil/NADPH oxidase, etc. | Inducing multiple inflammatory cytokines; NOS, COX, etc.: NO, PGs, etc. |
| TNF-α | | Inducing multiple inflammatory cytokines; NOS, COX, etc.: NO, PGs, etc. |
| Anticancer agents Heat | Vascular dilation | Gold nanoparticle or ferrite nanoparticle using electromagnetic, or laser, or microwave. |

such devices are not yet available in hospitals and may not have the right sensitivity at this time to detect the marker agent. The ability to image lymphatic function in the tumor vicinity could also provide a means to assess interstitial pressure imbalances. Efforts are underway to include dual-labeling PET for presurgical imaging and then NIR guidance during surgery (8). It is anticipated that PET will remain a crucial tool for clinical imaging and that the optical imaging counterpart will add value rather than being a replacement.

Ways to enhance the EPR effect in tumors were discussed and included drugs that impacted the vasculature (4)–for example, VEGF-based antagonists leading to vessel normalization, agents causing hypertension and increasing tumor blood flow, and agents that modulate the tumor matrix. Agents that generate nitric oxide [nitroglycerine or ISDN (isosorbide dinitrate)] were also shown to be effective in humans (4, 5). ACE inhibitor (e.g., enalapril), which potentiates the action of bradykinin, is also effective (4). Further work is required to validate the benefits of such agents in the context of exploiting the enhancement of EPR effect in the clinical setting (4, 5). It was suggested that both optimization of the nanoparticle and optimization of the tumor microenvironment were required for optimal delivery. Rakesh K. Jain (Harvard Medical School, Boston, Massachusetts); hypothesized that normalizing the vasculature, extracellular matrix, and lymphatics will lead to better delivery of drugs (9). However, normalized vasculature means that the average pore is smaller and this may require the use of smaller nanoparticles (~20 nm particle size). Overall, the

biologic impact of the abovementioned vascular effectors on delivery of nanoparticles of varying composition, shape, and flexibility needs significant further work.

The role of the lymphatics in tumor biology and nanoparticle delivery was discussed. This highlighted the need to consider changes in physiologic status, both in the acute and in long-term functionality of lymphatics in patients with cancer influenced by inflammation, tumor burden, or treatment. This is an area of active research and imaging techniques are being developed that will allow this to be explored in more detail.

In terms of animal tumor models to evaluate the EPR effect, subcutaneous flank tumor xenografts were thought to offer limited value. The vasculature of such models often resembles the vasculature found in very high EPR tumors, for example, renal tumors irrespective of tumor type, and thus probably gives a false impression about the benefit of nanoparticle-based drugs relying on the EPR effect in most tumor settings. The workshop participants felt that better options are provided by metastatic, orthotopic, and GEMM-based models, although these need further characterization and validation. Primary tumor explants may be another option to model delivery to tumor types with high stromal content. Further work is required to understand how to use the preclinical tumor models to investigate drugs relying on the EPR effect for activity and to understand how they reflect the heterogeneity seen in clinical disease. The site of the tumor was also considered to be important, and a more systematic assessment of vasculature architecture versus site of tumor was recommended.

Table 2. Survival benefits from the FDA-approved nanomedicines to date

| Generic drug | Trade name(s) | Indication | Benefit | | | | | | | | | | | | | |
|--|---------------------|------------------------------|---|-------------------------------------|--|--|--|------------|---------------------|---|--------|---------|------|---|------|---------|
| PEGylated liposomal doxorubicin | Doxil and Caelyx | HIV-related Kaposi's sarcoma | No statistically significant change in overall survival (23 wks) vs. doxorubicin, bleomycin, and vincristine treatment (22.3 wks) for HIV-related Kaposi's sarcoma | | | | | | | | | | | | | |
| | | Metastatic ovarian cancer | Statistically significant overall survival improvement (108 wks, $P = 0.008$) vs. topotecan treatment (71.1 wks) for platinum-sensitive patients with ovarian cancer | | | | | | | | | | | | | |
| | | Metastatic breast cancer | No statistically significant overall survival change (84 wks) vs. conventional doxorubicin (88 wks) for patients with breast cancer receiving first-line therapy | | | | | | | | | | | | | |
| Liposomal daunorubicin | DaunoXome | HIV-related Kaposi's sarcoma | No statistically significant overall survival change (52.7 wks) vs. doxorubicin, bleomycin, vincristine treatment (48.9 wks) | | | | | | | | | | | | | |
| Poly (styren-co-maleic acid)-conjugated naocarzinostat | SMANCS | Liver cancer, renal cancer | Approved in 1993 in Japan. Far more effective when the EPR is enhanced by increasing the blood pressure in difficult-to-treat tumors, including metastatic liver cancer, cancers of pancreas, gall bladder, etc. | | | | | | | | | | | | | |
| | | | <table border="1"> <thead> <tr> <th colspan="4">Liver cancer: 5-year survival (%)**</th> </tr> <tr> <th>Metastasis</th> <th>1 seg.⁺</th> <th>></th> <th>2 seg.</th> </tr> </thead> <tbody> <tr> <td>Child A</td> <td>>90%</td> <td>~</td> <td>>50%</td> </tr> <tr> <td>Child B</td> <td>40%</td> <td></td> <td>30%</td> </tr> </tbody> </table> <p>Five-year survival (%) based on the liver function (cirrhosis) by child classification and intrahepatic+ metastasis within one segment or more</p> | Liver cancer: 5-year survival (%)** | | | | Metastasis | 1 seg. ⁺ | > | 2 seg. | Child A | >90% | ~ | >50% | Child B |
| Liver cancer: 5-year survival (%)** | | | | | | | | | | | | | | | | |
| Metastasis | 1 seg. ⁺ | > | 2 seg. | | | | | | | | | | | | | |
| Child A | >90% | ~ | >50% | | | | | | | | | | | | | |
| Child B | 40% | | 30% | | | | | | | | | | | | | |
| Albumin-bound paclitaxel | Abraxane | Metastatic breast cancer | Statistically significant overall survival change (56.4 wks, $P = 0.024$) vs. polyethoxylated castor oil-based paclitaxel treatment (46.7 wks) for patients receiving second-line treatment | | | | | | | | | | | | | |

NOTE: The polymeric platform methoxy PEG-poly(D,L-lactide) taxol with the trade name Genexol-PM (Sanayang Co.) has been approved in Korea for the treatment of metastatic breast cancer. Adapted from the work of Jain and Stylianopoulos (16).

** , SMANCS data in the table were provided by H. Maeda.

Omid Farokhzad (Harvard Medical School) discussed the advantages of including a targeting agent on the nanoparticle to enhance the retention component and/or enable delivery of drug directly into the tumor cell via internalization of the nanoparticle. The majority of the currently available clinical data on nanoparticle oncology drugs relate to passively targeted liposomal drugs. Recently, several actively targeted nanoparticle products have also entered clinical development, including liposomes and polymeric particles containing payloads ranging from conventional cytotoxic drugs to genes expressing tumor suppressors (10). These particles are targeted to various tumor markers including the transferrin receptor HER-2 and prostate-specific membrane antigen (PSMA) using either protein or small-molecule ligands. Recent data were presented for BIND-014 (11), a

docetaxel-encapsulated polymeric nanoparticle targeted to PSMA, which is expressed on the surface of prostate cancer cells and nonprostate solid tumor neovasculature. In preclinical studies, BIND-014 increased the concentration of docetaxel in PSMA-expressing solid tumor xenografts by 5- to 10-fold. In a phase I clinical trial in patients with advanced solid tumors, BIND-014 displayed signals of antitumor efficacy in patients with advanced and metastatic cancer at low doses and in tumors where conventional docetaxel has minimal activity. With progress in polymeric nanoparticle engineering, similar approaches are also being applied to existing and developmental anticancer drugs, including other cytotoxics and molecularly targeted agents such as kinase inhibitors, and it will only be a matter of time before these advances will ultimately impact the treatment of cancer.

William Zamboni (University of North Carolina, Chapel Hill, North Carolina) characterized the pharmacologic properties of nanoparticles *in vivo* as part of preclinical and clinical studies. He stressed the importance of the MPS, tissue distribution, and potential tumor delivery on the clearance of nanoparticles. There is a bidirectional interaction between monocytes and liposomal agents and potentially other nanoparticle agents (12, 13). Monocytes internalize liposomes, which then releases the drug from the liposome and leads to toxic effects to the monocytes. The tissue distribution and tumor delivery of nanoparticles may involve MPS-mediated and non-MPS-mediated mechanisms where uptake of nanoparticles by circulating MPS cells compared with tumoral macrophages may result in different tumor drug exposure and responses. Dr. Zamboni has developed an *ex vivo* flow cytometry–based, high-throughput screening platform (HTSP) system called PhenoGLO-HTSP to measure the clearance of nanoparticles by the MPS and bidirectional interaction between the MPS and nanoparticles, conjugates, and antibody–drug conjugates. Importantly, this method also predicts nanoparticle pharmacokinetics and pharmacodynamics in humans where the MPS system seems to drive the clearance, efficacy, and toxicity of nanoparticle agents. PhenoGLO-IT can measure MPS function in a blood sample from patients as a method to individualize the dose of nanoparticle agents and/or as a biomarker for predicting pharmacokinetics and pharmacodynamics (response and toxicity) of nanoparticles.

The workshop participants felt that as our understanding of nanoparticle delivery to tumors increases, the emerging nanoformulations should be considered both as a general formulation strategy in drug development and as a selected strategy to improve delivery profiles of existing or failed drugs.

Prospects

During discussions at the conclusion of the symposium, participants recommended the formation of a working group to establish translational and clinical procedures for integrated clinical trials involving nanotherapeutic constructs and accompanying imaging approaches. Such translational studies and clinical trials would enable further understanding and predictability of EPR function in a tumor

and its primary or metastatic sites and may be critical for the development of future effective nanodrugs and predictive of antitumor response (14). An additional recommendation from this workshop was to generate a position paper highlighting key translational studies that should be conducted and parameters that should be monitored in nanoparticle drug delivery clinical trials to enable testing of various hypotheses for effective nanoparticle delivery (tumor perfusion, vascular permeability, interstitial penetration, retention, lymphatic function, MPS activity, blood pressure, fluid and solid stresses, others). In coming months, symposium participants will actively pursue these key recommendations and develop the necessary tools required to advance the scientific translation of the nanotechnology platform in the oncology therapeutic area.

Disclosure of Potential Conflicts of Interest

D.C. Blakey has ownership interest (including patents) in AstraZeneca. R.K. Jain is employed (other than primary affiliation; e.g., consulting) as a cofounder and board member of XTuit Pharmaceuticals, and as a board member of Hambrecht & Quist Healthcare Investors and Hambrecht & Quist Life Sciences Investors; has a commercial research grants from MedImmune, Roche, and Dyac; has ownership interest (including patents) in XTuit Pharmaceuticals; and is a consultant/advisory board member of Enlight Biosciences, SynDevRx, Dyac, Noxon Pharmaceuticals, and Zyngenia. E.M. Sevick-Muraca has ownership interest (including patents) in NIRFImaging, Inc. W. Zamboni has ownership interest (including patents) in PhenoGLO Technologies. O.C. Farokhzad has ownership interest (including patents) in and is a consultant/advisory board member of BIND Bioscience, Selecta Bioscience, and BLEND. A. Gabizon has a commercial research grant from Janssen Pharmaceuticals. No potential conflicts of interest were disclosed by the other authors.

Authors' Contributions

Conception and design: U. Prabhakar, D.C. Blakey, H. Maeda, R.K. Jain, E.M. Sevick-Muraca, O.C. Farokhzad, A. Gabizon, P. Grodzinski

Development of methodology: U. Prabhakar, P. Grodzinski

Acquisition of data (provided animals, acquired and managed patients, provided facilities, etc.): U. Prabhakar, P. Grodzinski

Analysis and interpretation of data (e.g., statistical analysis, biostatistics, computational analysis): U. Prabhakar, H. Maeda, P. Grodzinski

Writing, review, and/or revision of the manuscript: U. Prabhakar, D.C. Blakey, H. Maeda, R.K. Jain, E.M. Sevick-Muraca, W. Zamboni, O.C. Farokhzad, S. T. Barry, A. Gabizon, P. Grodzinski

Administrative, technical, or material support (i.e., reporting or organizing data, constructing databases): U. Prabhakar, H. Maeda, P. Grodzinski

Study supervision: U. Prabhakar, P. Grodzinski

Received December 14, 2012; revised February 7, 2013; accepted February 10, 2013; published OnlineFirst February 19, 2013.

References

1. Matsumura Y, Maeda H. A new concept for macromolecular therapeutics in cancer chemotherapy - Mechanism of tumorotropic accumulation of proteins and the antitumor agent smancs. *Cancer Res* 1986;46:6387-92.
2. Harisinghani MG, Barentsz J, Hahn PF, Deserno WM, Tabatabaei S, van de Kaa CH, et al. Noninvasive detection of clinically occult lymph-node metastases in prostate cancer. *N Engl J Med* 2003; 19:2491-9.
3. Gaglia JL, Guimaraes AR, Harisinghani M, Turvey SE, Jackson R, Benoist C, et al. Noninvasive imaging of pancreatic islet inflammation in type 1A diabetes patients. *J Clin Invest* 2011;121: 442-5.
4. Maeda H, Nakamura H, Fang J. The EPR effect for macromolecular drug delivery to solid tumors: improved tumor uptake, less systemic toxicity, and improved tumor imaging. *Review of the vascular permeability of tumors and the EPR effect. Adv Drug Deliver Rev* 2013;65:71-9.
5. Maeda H. Macromolecular therapeutics in cancer treatment: the EPR effect and beyond. *J Control Release* 2012;164:138-44.
6. Harrington KJ, Mohammadtaghi S, Uster PS, Glass D, Peters AM, Vile RG, et al. Effective targeting of solid tumors in patients with locally advanced cancers by radiolabeled pegylated liposomes. *Clin Cancer Res* 2001;7:243-54.
7. Sevick-Muraca EM. "Translation of near-infrared fluorescence imaging technologies: emerging clinical applications." *Annu Rev Med* 2012; 63:217-31.
8. Hall MA, Pinkston KL, Wilganowski N, Robinson H, Ghosh P, Azhdarinia A, et al. "Comparison of mAbs targeting EpCAM for detection of prostate cancer lymph node metastases with multimodal contrast: quantitative uPET/CT and NIRF imaging." *J Nucl Med* 2012;53: 1497-37.
9. Jain RK. Normalizing tumor microenvironment to treat cancer: Bench to bedside to biomarkers. *J Clin Oncol*. In press, 2013.

10. Kamaly N, Xiao Z, Valencia PM, Radovic-Moreno AF, Farokhzad OC. Targeted polymeric therapeutic nanoparticles: design, development and clinical translation. *Chem Soc Rev* 2012;41:2971–3010.
11. Hrkach J, Von Hoff D, Mukkaram Ali M, Andrianova E, Auer J, Campbell T, et al. Preclinical development and clinical translation of a PSMA-targeted docetaxel nanoparticle with a differentiated pharmacological profile. *Sci Transl Med* 2012;4:128ra39.
12. Caron WP, Rawal S, Song G, Kumar P, Lay JC, Zamboni WC. Bidirectional interaction between nanoparticles and cells of the mononuclear phagocyte system. In: Dobrovolskaia MA, McNeil SE, editors. *Immunological properties of Engineered Nanomaterials*. Singapore: World Scientific Publishing Co.; 2012.
13. Caron WP, Song G, Kumar P, Rawal S, Zamboni WC. Pharmacokinetic and pharmacodynamic disposition of carrier-mediated agents. *Clin Pharmacol Ther* 2012;91:802–12.
14. Petersen AL, Hansen AE, Gabizon A, Andresen TL. Liposome imaging agents in personalized medicine. *Adv Drug Deliv Rev* 2012;64:1417–35.
15. Fang J, Qin H, Nakamura H, Tsukigawa K, Maeda H. Carbon monoxide, generated by heme oxygenase-1, mediates the enhanced permeability and retention (EPR) effect of solid tumor. *Cancer Sci* 2012;102:535–41.
16. Jain RK, Stylianopoulos T. Delivering nanomedicine to solid tumors. *Nat Rev Clin Oncol* 2010;7:653.

Review Article

The link between infection and cancer: Tumor vasculature, free radicals, and drug delivery to tumors via the EPR effect

Hiroshi Maeda¹

Institute of Drug Delivery System Research, Sojo University, Kumamoto, Japan

(Received March 1, 2013/Accepted March 10, 2013/Accepted manuscript online March 16, 2013)

This review focuses primarily on my own research, including pathogenic mechanisms of microbial infection, vascular permeability in infection and tumors, and effects of nitric oxide (NO), superoxide anion radical (O_2^-), and 8-nitroguanosine in the enhanced permeability and retention (EPR) effect for the tumor-selective delivery of macromolecular agents (nanomedicines). Infection-induced vascular permeability is mediated by activation of the kinin-generating protease cascade (kallikrein-kinin) triggered by exogenous microbial proteases. A similar mechanism operates in cancer tissues and in carcinomatosis of the pleural and peritoneal cavities. Infection also stimulates O_2^- generation via activation of xanthine oxidase while generating NO by inducing NO synthase. These chemicals function in mutation and carcinogenesis and promote inflammation, in which peroxynitrite (a product of O_2^- and NO) activates MMP, damages DNA and RNA, and regenerates 8-nitroguanosine and 8-oxoguanosine. We showed vascular permeability by using macromolecular drugs, which are not simply extravasated through the vascular wall into the tumor interstitium but remain there for prolonged periods. We thus discovered the EPR effect, which led to the rational development of tumor-selective delivery of polymer conjugates, micellar and liposomal drugs, and genes. Our styrene-maleic acid copolymer conjugated with neocarzinostatin was the first agent of its kind used to treat hepatoma. The EPR effect occurs not only because of defective vascular architecture but also through the generation of various vascular mediators such as kinin, NO, and vascular endothelial growth factor. Although most solid tumors, including human tumors, show the EPR effect, heterogeneity of tumor tissue may impede drug delivery. This review describes the barriers and countermeasures for improved drug delivery to tumors by using nanomedicines. (*Cancer Sci*, doi: 10.1111/cas.12152, 2013)

As the recipient of the Tomizo Yoshida Award of the Japanese Cancer Association in 2011, I herein describe my personal recollections of my research. This review covers the pathogenic mechanisms of microbial infection and generation of endogenous bradykinin (also called kinin) and free radicals O_2^- and NO in bacterial and viral infections. This review also discusses selective delivery of anticancer macromolecular agents (now called nanomedicines) to tumor tissue, which take advantage of the vascular permeability of tumor tissue (analogous to inflamed tissue). Projects involving the antitumor antibiotic protein neocarzinostatin (NCS, 13 kDa) were pursued in my laboratory at the Department of Microbiology, Kumamoto University School of Medicine (Kumamoto, Japan) for more than two decades,⁽¹⁻³⁾ and this research led me to the field of nanomedicine.

Around 1978, my research focused on developing an antitumor agent that would target metastatic tumors, or more specifically, to target to the lymphatic system. For this purpose, I had to design an anticancer agent with lipophilic and macromolecular characteristics, because these features would favor preferential recovery of the agent through the lymphatic system from lymphatic networks in the interstitial space after extravasation from blood vessel lumina. In 1978, therefore, I prepared a conjugate of NCS with SMA, in which SMA conferred lipophilic and polymeric characteristics.⁽¹⁻³⁾ This agent was the first polymer-conjugated macromolecular anticancer drug, named SMANCS, and was reported as the first macromolecular anticancer agent having antimetastatic activity.⁽⁴⁻⁸⁾ SMANCS possessed many advantages including lipid formulation using Lipiodol[®],⁽⁹⁾ as described later, and also effective to the multidrug resistance of tumor cells.⁽⁸⁻¹¹⁾

Thereafter, we carried out more detailed pharmacological studies of SMANCS and other macromolecular drugs, including plasma proteins and synthetic polymers, which led to the discovery of the unique pharmacokinetics of polymeric drugs and, more importantly, the EPR effect.^(5-8,12-15) We then investigated the EPR effect in greater detail and found that many vascular mediators, such as bradykinin (also called kinin), NO, ONOO⁻, prostaglandins, vascular endothelial growth factor, collagenase, and more recently, carbon monoxide, are responsible for this effect (Table 1).⁽¹⁵⁻²²⁾ Our earlier studies of the kinin-generating cascade triggered by microbial proteases and biological generation of free radicals in infection were quite useful for understanding these vascular mediators and the EPR effect and for developing methods to further augment cancer drug delivery based on the EPR effect. The ultimate outcome of these studies can provide theoretical mechanism, and extend to the application of nanomedicines for tumor selective delivery to treat cancer in the future.

Relation of vascular permeability to infection and cancer: Inflammatory mediators in bacterial infection and cancer

We first discovered that kinin, the most potent pain-inducing endogenous peptide hormone, was generated by exogenous bacterial proteases through the activation of one or more steps in the kinin-generating cascade, which begins with stimulation of Hageman factor, or factor XII (which would lead to the blood coagulation cascade), and continues to involve prekallikrein to kallikrein (Fig. 1), and then generation of kinin from

¹To whom correspondence should be addressed.
E-mail: hirmaeda@ph.sojo-u.ac.jp
This manuscript is a Tomizo Yoshida award lecture.

Table 1. Factors affecting the enhanced permeability and retention (EPR) effect of macromolecular drug delivery to solid tumors

| Mediators† | Responsible enzymes and mechanisms‡ | References |
|--|---|-------------|
| Bradykinin | Kallikrein/protease | 16,19,32,33 |
| NO | iNOS | 17,18,96 |
| VPF/VEGF | Involved in NO generation | 76,77 |
| Prostaglandins | Cyclooxygenase-1 | 76,77,95 |
| Collagenase (proMMPs → MMP) | Activated from proMMPs by peroxynitrite or proteases | 20 |
| Peroxyntirite (ONOO ⁻) | NO + O ₂ ⁻ → ONOO ⁻ → proMMP → MMP | 20 |
| Carbon monoxide | Heme oxygenase-1 | 97 |
| Induced hypertension | Using angiotensin II | 70,77,89 |
| Inflammatory cells and H ₂ O ₂ | Neutrophil/NADPH oxidase, etc. | |
| Transforming growth factor-β inhibitor | | 114 |
| Vascular endothelial cell growth factor (VEGF) | Also involves NO | 77,93 |
| Tumor necrosis factor-α | | 115 |
| Anticancer agents | | |
| Heat | | 116 |

†Extensive production of vascular mediators that facilitate extravasation from normal and tumor vessels. ‡Enzymes or mechanisms involved in each process (see text for details). iNOS, inducible form of nitric oxide synthase; NO, nitric oxide; VEGF, vascular endothelial growth factor; VPF, vascular permeability factor.

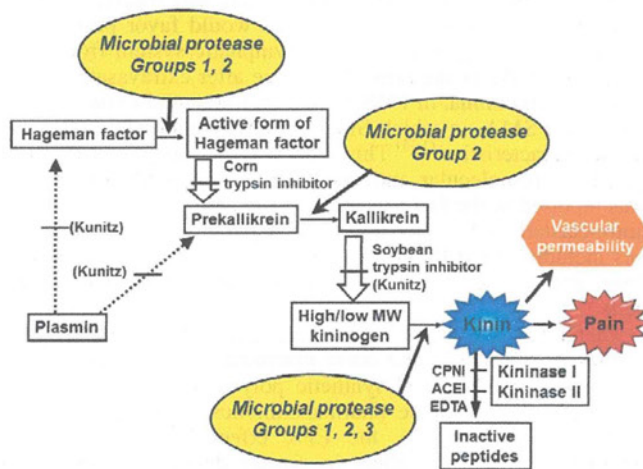


Fig. 1. Kinin-generating cascade activated by proteases, which begins with activation of Hageman factor (factor XII), continues to prekallikrein and kallikrein, then yields kinin (blue). Kinin stimulates vascular leakage (permeability). Tumor tissue has a more active cascade, which thus produces excessive kinin. Corn trypsin inhibitor, soybean trypsin inhibitor, and carboxypeptidase N inhibitor (CPNI) can inhibit this cascade. ACEI, angiotensin-converting-enzyme inhibitor; MW, molecular weight.

high- and low-molecular-weight kininogen in blood plasma. All pathogenic bacterial and fungal infections induce inflammation,⁽²³⁻²⁵⁾ in which extravasation of plasma proteins is a hallmark event and causes edema and in which bradykinin is a key mediator. Similar such events were later found to occur in solid tumors. We have discovered no effective inhibitor in the body against all microbial proteases, including fungal protease, that we tested.⁽²⁶⁻³¹⁾

With regard to cancer, we found a significantly high concentration of kinin, which was generated by the above-mentioned mechanism, in blood plasma and in peritoneal or pleural carcinomatosis in tumor-bearing hosts including humans.⁽³²⁻³⁴⁾ Kinin generation was effectively inhibited by inhibitors of kallikrein such as soybean trypsin inhibitor or by kinin antagonists.⁽³²⁻³⁴⁾

Various tumor cells highly express bradykinin receptors, which lead to growth stimulation, angiogenesis, metastasis, and release of MMPs involving NO, prostaglandins, and vari-

ous other cytokine signaling pathways.⁽³⁵⁻³⁸⁾ We focused our attention, however, on vascular permeability in tumors and delivery of macromolecular drugs that was given i.v., which led to discovery of the EPR effect.

Wu and others in our department showed that the kinin antagonist HOE 140 (Hoechst, Frankfurt, Germany) or kallikrein inhibitors, such as soybean trypsin inhibitor, can block this extravasation of plasma proteins in cancer tissue.^(19,20) Soybean trypsin inhibitor and other serine protease inhibitors (such as PMSF) effectively suppressed formation of peritoneal and pleural ascites,⁽³²⁻³⁴⁾ in which the kinin concentration was quite high, and facilitated fluid accumulation.^(16,32,33) Kinin antagonists were later found to suppress tumor growth, thus they may be good therapeutic targets in cancer therapy and pain control.^(37,38) However, the involvement of bradykinin in tumor biology and pathogenesis warrants further investigation.

My experiences with protein anticancer drugs, that is, NCS and SMANCS, therefore made me realize, in the early 1980s, the potential use of the enhanced vascular permeability of solid tumors for delivery of macromolecular anticancer drugs.⁽³⁶⁻³⁸⁾

Endogenous free radical generation in infection: A significant cause of tissue damage by O₂⁻ and mutation

We focused on two research areas of infectious diseases: one was exogenous bacterial proteases, which involve the kinin cascade and degenerative tissue damage; and the other was biological free radicals, that is, ROS and RNS, as derived from NO. We first found that O₂⁻ was generated in excess during respiratory infection with influenza virus in mice.^(39,40) Our initial hypothesis, that Nox of infiltrated leukocytes would play a major role, was determined to be untrue. Instead, the major source of O₂⁻ generation was excessive activation of XO to about 400-fold from xanthine dehydrogenase. This enzyme is involved in the latter part of adenosine catabolism: adenosine → inosine → hypoxanthine → xanthine → uric acid + 2 × O₂⁻; in this cascade, adenosine deaminase activity increased approximately 170-fold,⁽³⁹⁻⁴²⁾ and Nox was second in importance.

Our discovery of excessive generation of O₂⁻ in viral infection was an unprecedented finding that was proved by means of three completely different methods. The first used pyran copolymer-conjugated SOD, which removed O₂⁻ and markedly improved the survival rate (Fig. 2a). The polymer-SOD conjugate was designed to have a plasma half-life more than 100 times longer than that of native SOD, which is cleared from

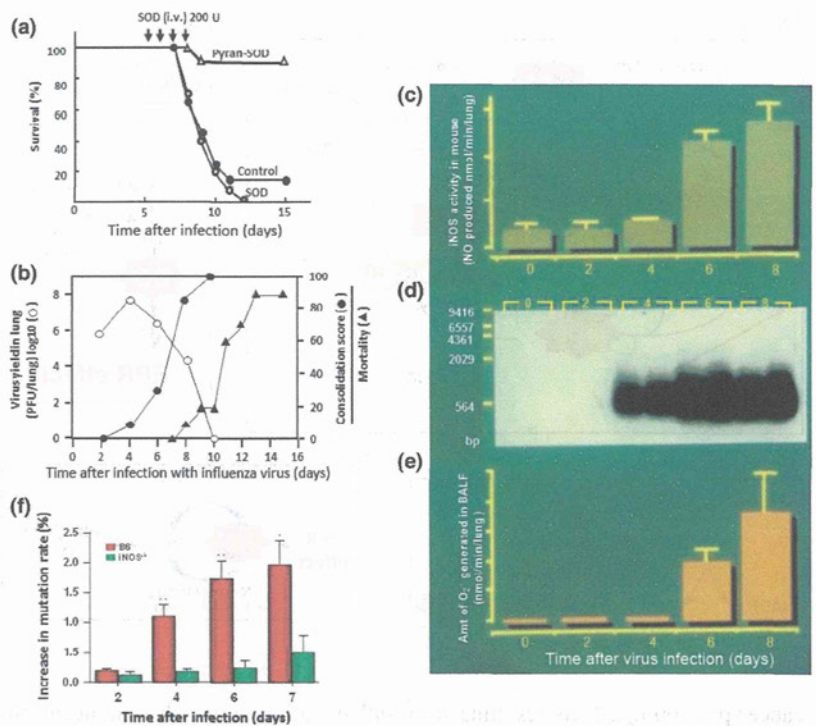


Fig. 2. Pathological and molecular events in influenza virus-infected mice. (a) Treatment of influenza virus-infected mice with native superoxide dismutase (SOD) (○), polymer (pyran)-conjugated SOD (Δ), or no drug (control) (●). (b) Time course of virus yield (○), consolidation score (●), and mortality (▲). All these events occurred separately. (c–e) Activity of the inducible form of nitric oxide synthase (iNOS) and superoxide (O₂⁻). (c) iNOS activity. (d) Induction of PCR-detectable iNOS mRNA. (e) Amount of O₂⁻ generated after virus infection. (f) Effect of mutant virus formation in wild-type iNOS⁺ B6 mice (red bars) and iNOS^{-/-}B6 transgenic mice (green bars). More mutant virus was formed in NO-generating wild-type mice, which indicated a need for NO for viral mutation. BALF, bronchoalveolar lavage fluid.

the blood circulation in mice within a few minutes.^(39,40) This conjugate was likely the first polymer-conjugated therapeutic enzyme, the idea for which derived from our experience with SMANCS, as described in more detail later.

The second method used the XO inhibitor allopurinol, which improved the survival rate of virus infected mice in a dose-dependent manner. The third was injection of adenosine, which generates inosine and then hypoxanthine (a substrate of XO) and O₂⁻, which itself facilitated a pathogenic effect and resulted in severe exacerbation of this viral infection and an accelerated death rate of mice.^(39–41)

During influenza virus infection, the amount of virus (i.e. virus yield), consolidation score of the lung, and mortality rate of infected mice increased, but not simultaneously. Figure 2(b) illustrates that the amount of virus in the alveolar compartment, as determined by bronchoalveolar lavage, was highest on day 4 after infection then decreased to undetectable levels on day 10, whereas pathological manifestations as indicated by the consolidation score and O₂⁻ generation started to increase on day 6 and reached a maximum on day 10, when the mice started to die and virus was no longer detectable.^(39–41) Thus, all three events occurred separately, not simultaneously, and I coined the phrase “virus disease in the absence of virus,” for situations in which the amount of virus did not completely correspond to pathological severity.⁽⁴²⁾

As another important finding, the data showed that oxygen radicals (ROS) can be generated by a truly biological event as a host response *in vivo*, not just by intense UV irradiation, X-ray, or γ -ray exposure *in vitro*. That the generation of free radicals is clearly an etiological principle in infectious diseases can also be stated. In other words, this pathological mechanism extends beyond the boundary of Robert Koch’s postulate or paradigm.⁽⁴²⁾ This mechanism will also offer alternative therapeutic options against infectious diseases by using scavengers of O₂⁻ (Fig. 2a) or by inhibiting ROS-generating systems that will reduce the pathogenic potential and cure diseases.

We subsequently found that another biological free radical, NO, is excessively generated under conditions similar to

those of influenza virus infection (Fig. 2c–e), which also possesses a pathogenic potential.^(43–48) That O₂⁻ and NO react rapidly and form ONOO⁻, which is an agent with extremely potent oxidizing and nitrating activities occurring simultaneously, is well known. ONOO⁻ would therefore modify DNA and RNA by nitration or oxidation, or by strand breaks (Fig. 2f).^(43–50) This increased mutation by ROS and RNS was also shown in bacteria^(49,50) as well as influenza and Sendai viruses,^(44,47,48) and antioxidant scavengers suppressed mutagenesis and carcinogenesis.^(49–52) These data support the idea that carcinogenesis induced by infection and inflammation would proceed through free radical generation or oxidative stress.^(51,52)

Furthermore, a finding relevant to free radical-induced carcinogenesis is that 8-nitroguanosine becomes a substrate for NOS. Also, the NADPH reductase, cytochrome b5 reductase, and reductase domain of NOS similarly generate O₂⁻ (Fig. 3a).^(53–57) In separate but related studies, we showed that various heterocyclic amines (all 11 kinds) and NCS effectively produced O₂⁻. All these chemicals are mutagens in the presence of NADPH and cytochrome P450 reductase (Fig. 3b).^(53–56) Also, the mutation rate of *Salmonella typhimurium* (Ames strains) paralleled to the amount of O₂⁻ produced.⁽⁵⁷⁾

We collaborated with Dr. Tatematsu of Aichi Cancer Center Research Institute (Nagoya, Japan) in studies of our novel phenolic antioxidant compound named canolol, which suppressed *Helicobacter pylori*-induced inflammation, ONOO⁻ cytotoxicity, and carcinogenic potential, whereas canolol did not affect the number (colony-forming units) of *H. pylori* bacilli.^(49–51) These data support the proposal that free radical generation is a key process in the mediation of inflammation and chemical carcinogenesis, as previously expected.⁽⁵²⁾ Additional details about the chemical damage to nucleic acids by ONOO⁻ have been provided by Niles *et al.*,⁽⁵⁸⁾ Sawa and Ohshima,⁽⁵⁹⁾ and others.

In view of the relation among inflammation, oxidative damage, and carcinogenesis, Okada, Kobayashi, Tanaka, Cao, Shimizu, Muto, Surh, and many others showed the potent

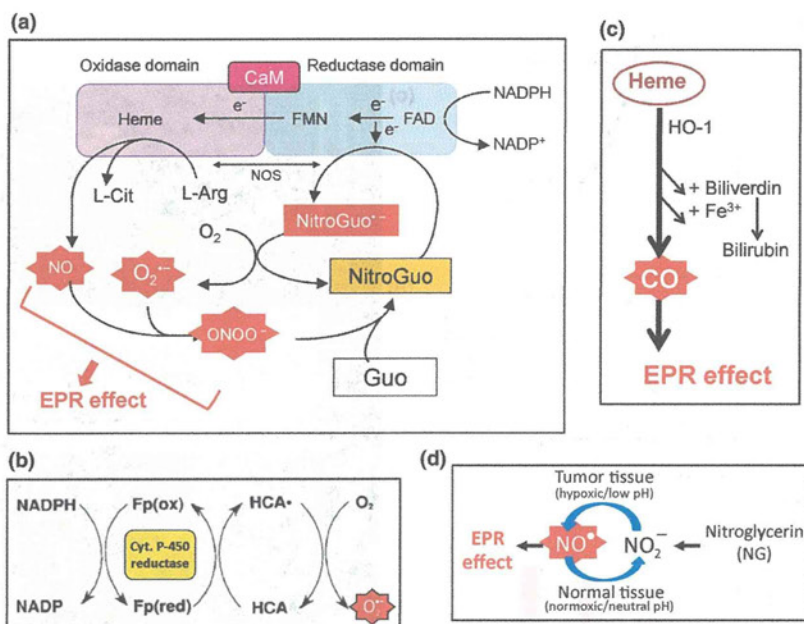


Fig. 3. Generation of free radicals in infection and cancer. (a) Nitric oxide synthase (NOS) can generate nitric oxide (NO) and superoxide (O_2^-), and then peroxyntirite ($ONOO^-$) can nitrate guanine (\rightarrow 8-nitroguanine), and 8-nitroguanine (NitroGuo) can become a substrate of NOS or cytochrome c reductase, thereby generating O_2^- . The total system thus works as a progressive reaction, with a stoichiometry of greater than 1:1. (b) Generation of O_2^- from heterocyclic amine (HCA) in the presence of cytochrome (Cyt.) P450 reductase and NADPH, which results in DNA damage or cleavage and mutation.^(53–55,57) (c) Heme oxygenase (HO-1) can generate carbon monoxide (CO), which results in the enhanced permeability and retention (EPR) effect. HO-1 is usually upregulated in most tumors. (d) Enhancement of the EPR effect by application of nitroglycerin. FAD, flavin adenine dinucleotide; FMN, flavin mononucleotide; fp(ox), flavoprotein oxidized form; fp(red), flavoprotein reduced form.^(90,96)

cancer-promoting effects resulting from inflammation, in which the oxygen burst caused by Nox and the NO generation induced by iNOS derived from infiltrated leukocytes^(51,60–67) were crucial requirements. This concept has now become a textbook example of an essential component of carcinogenesis, including that in humans.⁽⁶⁸⁾

Vascular permeability leading to tumor-targeted drug delivery, lymphotropism, and mechanism of the EPR effect of macromolecules

Uniqueness of tumor vasculature, and extravasation of macromolecules given i.v. As mentioned earlier, we simultaneously carried out multiple research projects in my laboratory. The anticancer agent composed of a conjugate of a polymer (SMA) and a protein (NCS) (i.e. SMANCS) showed considerable lymphotropic accumulation, consequently it became effective against metastatic tumors in rats.^(12–4,6–8) Another important finding was the markedly high accumulation of SMANCS in tumor tissues, as we expected,^(5–8,69,75–78) which was approximately 10–100 times greater than that in normal tissues (Fig. 4). We also found that the plasma concentration (or AUC) of SMANCS at 24 h after i.v. inoculation in both mice and patients was more than 20 times greater than that of the parent drug NCS.

To understand the mechanism underlying this tumoritropic behavior of biocompatible macromolecules and SMANCS, we carried out additional investigations with biocompatible macromolecules such as albumin (68 kDa), transferrin (90 kDa), and IgG (160 kDa) as well as small proteins (NCS, 13 kDa, and ovomucoids, 29 kDa).^(5,6) The results showed a progressive increase in accumulation of large proteins in solid tumors over time. Concentrations of these proteins in most tumors strikingly exceeded their concentrations in blood. Also, drug accumulation in tumors paralleled the AUC for macromolecules.^(5,12–15) SMANCS (16 kDa), which binds with plasma albumin (resulting in a size of 90 kDa) manifested tumoritropic characteristics, and we proposed a new concept of tumor-selective drug delivery based on the EPR effect (Fig. 4).^(5,6,15,69) In this concept, tumor uptake of drugs is not transitory, as observed by angiography for low-

molecular-weight contrast agents; instead, tumor tissues show persistent retention of macromolecules for a very long time, for example, many weeks.

To elucidate the EPR effect, we collaborated with Duncan, Ulbrich, and others and used the well-characterized biocompatible P-HPMA, whose size ranged from 4.5 kDa to 800 kDa and had a neutral charge.^(12–15) As a putative macromolecular drug, P-HPMA showed progressive accumulation in tumor tissue (Fig. 4f). The EPR effect, therefore, results in little delivery of macromolecular drugs to normal tissues and thus fewer systemic toxic effects compared to the delivery of low-molecular-weight drugs,^(69,70) which have no tumor selectivity. Kimura *et al.* reported that i.v.-injected *Bifidobacterium bifidum*, with a size $>1 \mu\text{m}$, accumulated preferably in tumor tissue compared with other normal tissues.⁽⁷¹⁾ Subsequently, we and Skinner *et al.* showed that polymer resin of acrylamide that was given i.v. extravasated into interstitial tissue of solid tumor.^(72–75)

In addition, we observed the EPR effect in small (200- μm diameter) tumor nodules in liver that were metastatic from colon cancer (Fig. 4d).^(72–74) Numerous laboratories have now reported on the EPR effect, and as of 2012 more than 12 000 published reports cited our own papers on this matter.^(76–79)

Clinical demonstration of vascular permeability and the EPR effect after arterial infusion of SMANCS/Lipiodol. The classic example of the clinical demonstration of the EPR effect may be gallium scintigraphy, in which radioactive ^{67}Ga citrate is injected i.v.⁽⁸⁰⁾ We now interpret this finding to indicate that the gallium ion forms a complex with the plasma protein transferrin, thereby becoming a 90-kDa macromolecule *in vivo*. Consequently, because of the EPR effect, the tumor-selective accumulation of radioactive ^{67}Ga would produce a distinct tumor image in a day or two after i.v. injection, as seen by radiosintigraphy.

We also found that CT obtained striking tumor images after a lipidic radiocontrast agent, Lipiodol[®] (a product of Laboratoire Guerbet, France, which is iodinated poppy seed oil ester), was injected into the tumor-feeding artery, as discussed blow (Fig. 4e, e'). This result is clearly based on the EPR effect.^(1,75,77,82–86)

Shortly after biochemical, physical, and preclinical characterizations of SMANCS were completed, our colleagues at Kumamoto University were quite fascinated with its tumor